Electronic Supplementary Material (ESI) for New Journal of Chemistry.
This journal is © The Royal Society of Chemistry and the Centre National de la Recherche Scientifique 2021

Multi-stimuli responsive property and structure-property study of tetraphenylethylene functionalized arylimidazole derivatives

Shengmei Guo[a], Gaobin Zhang[*ab], Fangjie Chen[b], Yingyong Ni[a], Jianyan Huang[a], Lin Kong[a], Jiaxiang Yang[*a]

[a]*College of Chemistry and Chemical Engineering, Key Laboratory of Functional Inorganic Materials of Anhui Province, Anhui University, Hefei 230601, P. R. China*

[b] *Henan Key Laboratory of Materials on Deep-Earth Engineering, School of Materials Science and Engineering, Henan Polytechnic University, Shiji road 2001, Jiaozuo 454003, P. R. China.*

**Corresponding authors. E-mail address: jxyang@ahu.edu.cn*

1. Materials and instruments

All of the chemicals and solvents were obtained from commercial suppliers without further purification. ^{1}H and ^{13}C NMR spectra of tetraphenylethylene derivatives containing arylimidazole unit were acquired with a Bruker Avance 400 NMR spectrometer using $CDCl_3$ as solvent. Mass spectrometry (MS) analyses were investigated on LTQ Orbitrap spectrometer. FT-IR spectra were collected from using the KBr pellet method on a Nicolet 380. The UV-vis absorption spectra were carried out with a TU-1901 spectrophotometer (Japan). PL measurements at room temperature were obtained on a Hitachi FL-7000 spectrometer from Hitachi High Technologies Corporation (Tokyo, Japan). Dynamic Light Scattering (DLS) measurements were recorded on a Malvern Zetasizer Nano ZS90 size analyzer. The time-resolved PL decay spectra and absolute FL quantum yields of the samples were also performed on a HORIBAFluoroMax-4P fluorescence spectrometer at room temperature (R. T.). Quantum yield (Φ_{PL}) was measured by calibrated integrating sphere. The digital photographs were captured by a Nikon D7000 camera. Powder X-ray diffraction (PXRD) experiments were examined using a MXP18AHF diffractometer (Japan). Scanning electron microscope (SEM) images were taken on a scanning electron microscope (Jeol JSM-4800, Japan). Thermogravimetry (TG) was performed using TGA5500 and differential scanning calorimetry (DSC) was measured at a heating rate of 10 °C/min under N_2 atmosphere using DSC apparatus (MET-TLER82le/40).

2. **Synthesis of compound G4**, **G3**, **G2**.

Compound **G4**: Benzil (1.00 g, 4.76 mmol) and pyridine-4-carboxaldehyde (943 mg, 7.14 mmol) were dissolved in anhydrous acetic acid (30 mL) at room temperature. 2-(4-aminophenyl) acetonitrile (662 mg, 5.71 mmol) was dissolved in glacial acetic acid (5 mL) and was gradually added into this mixture solution. The mixture was stirred for 2 h at 25 °C. Then, ammonium acetate (1.83 g, 23.78 mmol) was added and the mixture was heated to 120 °C for 12 h. The coarse product was poured into brine

(200 mL) and was neutralized with NaOH aqueous solution. The coarse product (477 mg, 1.16 mmol) and 4-(1,2,2-triphenylvinyl)benzaldehyde were uniformly dispersed in ethanol (20 mL) at 80 °C. Soon afterwards, t-BuOK (195 mg, 1.73 mmol) was added. The reaction mixture was refluxed for 5 h. The final mixture was poured into brine (200 mL). The generated green precipitate was filtered and further purified by column chromatography (petroleum ether: dichloromethane (1 : 1, v/v) to afford compound **G4** (620 mg, 821 μmol). Yield: 70%. FT-IR (cm^{-1}, KBr) *v*: 3050, 3029, 2923, 2851, 2218, 1597, 1518, 1419, 1025, 858, 823, 748, 700, 577, 545, 503. ^{1}H NMR ($CDCl_3$, 400 MHz) δ (ppm): 8.52-8.50 (m, 2H), 7.65 (d, J = 8.4 Hz, 2H), 7.60-7.57 (m, 4H), 7.42 (s, 1H), 7.32 (d, J = 6.2 Hz, 2H), 7.31-7.27 (m, 4H), 7.25-7.21 (m, 1H),7.15-7.09 (m, 16H), 7.06-7.01 (m, 6H). ^{13}C NMR ($CDCl_3$, 100 MHz) δ (ppm): 149.92, 147.21, 143.24, 143.08, 142.68, 139.90, 139.46, 137.58, 136.99, 135.23, 133.76, 132.27, 132.04, 131.35, 131.28, 131.14, 131.04, 129.77, 128.96, 128.83, 128.70, 128.62, 128.33, 127.92, 127.72, 127.34, 127.12, 126.98, 126.81, 126.79, 122.44, 117.72, 108.99. APCI-MS: m/z $[M+H]^+$ calcd for $C_{55}H_{39}N_4$: 755.3175, found = 755.3188.

Compound **G3**: replace pyridine-4-carboxaldehyde with pyridine-3-carboxaldehyde. Yield: 68%. FT-IR (cm^{-1}, KBr) *v*: 3056, 3024, 2927, 2853, 2218, 1602, 1513, 1445, 1074, 1026, 851, 750, 699, 616, 571. ^{1}H HMR ($CDCl_3$, 400 MHz) δ (ppm): 8.62 (s, 1H), 8.52 (d, J = 4.84, 1H), 7.82 (d, J = 8.00, 1H), 7.63-7.53 (m, 6H), 7.38 (s, 1H), 7.29-7.21 (m, 7H), 7.16-7.09 (m, 15H), 7.06-7.01 (m, 6H). ^{13}C NMR ($CDCl_3$, 100 MHz) δ (ppm): 149.52, 149.26, 147.08, 144.01, 143.25, 143.15, 143.07, 142.60, 139.91, 139.16, 136.98, 136.08, 135.00, 133.91, 132.00, 131.43, 131.35, 131.31, 131.26, 131.16, 131.04, 129.98, 128.91,128.84, 128.65, 128.47, 128.29, 127.99, 127.70, 127.33, 126.99, 126.95, 126.78, 126.73, 126.60, 123.15, 117.70, 109.04. APCI-MS: m/z $[M+H]^+$ calcd for $C_{55}H_{39}N_4^+$: 755.3175, found: 755.3163.

Compound **G2**: replace pyridine-4-carboxaldehyde with pyridine-2-carboxaldehyde. Yield: 78%. FT-IR (cm^{-1}, KBr) *v*: 3056, 3024, 2927, 2853, 2218, 1602, 1513, 1445, 1074, 1026, 851, 750, 697, 642, 616, 574. ^{1}H HMR ($CDCl_3$, 400 MHz) δ (ppm): 8.29 (d, J = 4.84 Hz, 1H), 8.06 (d, J = 7.92 Hz, 1H), 7.71 (t, J = 7.72

Hz, 1H), 7.61 (t, *J* = 8.44 Hz, 4H), 7.49 (d, *J* = 8.60 Hz, 2H), 7.37 (s, 1H), 7.27-7.22 (m, 6H), 7.16-7.10 (m, 16H), 7.06-7.02 (m, 6H). ^{13}C NMR ($CDCl_3$, 100 MHz) δ (ppm): 149.59, 148.67, 146.79, 145.55, 143.28, 143.12, 142.50, 142.37, 139.96, 138.73, 128.41, 136.38, 134.18, 133.89, 131.96, 131.40, 131.35, 131.32, 131.28, 131.15, 130.25, 128.94, 128.82, 128.54, 128.31, 128.19, 127.90, 127.71, 127.39, 126.93, 126.81, 126.76, 125.84, 123.84, 122.77, 117.92, 109.61. APCI-MS: m/z $[M+H]^+$ calcd for $C_{55}H_{39}N_4$: 755.3175, found: 755.3170.

3. Synthesis of compound L-G4, **L-G3**, **L-G2**.

Compound **L-G4**: phenanthraquinone (1.00 g, 4.76 mmol) and pyridine-4-carboxaldehyde (943 mg, 7.14 mmol) were dissolved in anhydrous acetic acid (30 mL) at room temperature. 2-(4-aminophenyl) acetonitrile (662 mg, 5.71 mmol) was dissolved in glacial acetic acid (5 mL) and was gradually added into this mixture solution. The mixture was stirred for 2 h at 25 °C. Then, ammonium acetate (1.83 g, 23.78 mmol) was added and the mixture was heated to 120 °C for 12 h. The coarse product was poured into brine (200 mL) and was neutralized with NaOH aqueous solution. To a flask containing coarse product (477 mg, 1.16 mmol) was added 4-(1,2,2-triphenylvinyl)benzaldehyde (500 mg, 1.39 mmol), t-BuOK (195 mg, 1.73 mmol) and EtOH (20 ml) at 80 °C. The reaction mixture was refluxed for 5 h. The final mixture was poured into brine (200 mL). The generated green precipitate was filtered and further purified by column chromatography (petroleum ether: dichloromethane (1 : 1, v/v) to afford compound **L-G4** (590 mg, 782 μmol). Yield: 68%. FT-IR (cm^{-1}, KBr) *v*: 3057, 3027, 2923, 2853, 2231, 2216, 1596,1508, 1491, 1454, 1418, 1385, 1071, 1031, 994, 899, 856, 825, 757, 747, 725, 701, 673, 642, 614, 572. ^{1}H NMR ($CDCl_3$, 400 MHz) δ (ppm): 8.84 (d, *J* = 8.00 Hz, 1H), 8.77 (d, *J* = 7.84 Hz, 1H), 8.69 (d, *J* = 8.04 Hz, 1H), 8.56-8.54 (m, 2H), 7.93-7.91 (m, 2H), 7.77-7.73 (m, 3H), 7.70-7.65 (m, 1H),7.62-7.59 (m, 3H), 7.57-7.53 (m, 1H), 7.46-7.45 (m, 2H), 7.33-7.29 (m, 1H), 7.22-7.10 (m, 13H), 7.08-7.02 (m, 5H). ^{13}C NMR ($CDCl_3$, 100 MHz) δ (ppm): 150.09, 147.70, 147.54, 143.97, 143.32, 143.15, 142.86, 139.97, 138.66, 138.01, 137.83, 136.81, 132.21, 131.45, 131.37, 131.18, 129.87, 129.64, 129.21, 128.92, 128.59, 128.03, 127.83, 127.69, 127.10, 127.04, 126.93, 126.28,

125.75, 124.43, 123.30,122.97, 122.86, 122.71, 120.94, 117.87, 108.97. APCI-MS: m/z $[M+H]^+$ calcd for $C_{55}H_{39}N_4$: 753.3018, found = 753.3075.

Compound **L-G3**: replace pyridine-4-carboxaldehyde with pyridine-3-carboxaldehyde. Yield: 69%. FT-IR (cm^{-1}, KBr) *v*: 3051, 3027, 2919, 2854, 2216, 1598, 1576, 1514, 1489, 1453, 1419, 1381, 1147, 1075, 1023, 852, 752, 726, 699, 616, 571, 545. ^1H NMR ($CDCl_3$, 400 MHz) δ (ppm): 8.84 (d, J = 8.0 Hz, 1H), 8.79-8.75 (m, 2H), 8.71 (d, J = 8.3 Hz, 1H), 8.55 (d, J = 4.9 Hz, 1H), 7.94-7.92 (m, 1H), 7.87 (d, J = 8.5 Hz, 2H), 7.77-7.65 (m, 4H), 7.59-7.53 (m, 4H), 7.33-7.21 (m, 3H), 7.17-7.02 (m, 17H). ^{13}C NMR ($CDCl_3$, 100 MHz) δ (ppm): 149.91, 149.84, 148.06, 147.45, 143.94, 143.33, 143.16, 142.81, 140.00, 138.62, 137.95,136.72, 136.64, 132.19, 131.46, 131.38, 131.22, 129.73, 129.64, 129.17, 128.51, 128.04, 127.81, 127.78, 127.62, 127.09, 126.91, 126.80, 126.67, 126.12, 125.51, 124.39, 123.31, 122.81, 122.76, 120.88, 117.86, 109.03. APCI-MS: m/z $[M+H]^+$ calcd for $C_{55}H_{37}N_4$: 753.3018, found = 753.3091.

Compound **L-G2**: replace pyridine-4-carboxaldehyde with pyridine-2-carboxaldehyde. Yield: 62%. FT-IR (cm^{-1}, KBr) *v*: 3051, 3024, 2922, 2852, 2214, 1584, 1513, 1493, 1454, 1438, 1424, 1385, 1280, 1152, 1075, 1030, 996, 851, 790, 735, 725, 614, 576, 548. ^1H HMR ($CDCl_3$, 400 MHz) δ (ppm): 8.87 (d, J = 8.4 Hz, 1H), 8.77 (d, J = 7.76 Hz, 1H), 8.70 (d, J = 8.20 Hz, 1H), 8.34-8.32 (m, 1H), 8.19 (d, J = 7.92 Hz, 1H), 7.82 (d, J = 8.6 Hz, 2H), 7.77-7.71 (m, 4H), 7.68-7.67 (m, 1H), 7.61-7.58 (m, 3H), 7.55-7.51 (m, 1H), 7.31-7.27 (m, 1H), 7.21-7.02 (m, 19H). ^{13}C NMR ($CDCl_3$, 100 MHz) δ (ppm): 149.52, 149.26, 147.08, 144.01, 143.25, 143.15, 143.07, 142.60, 139.91, 139.16, 136.98, 136.08, 135.00, 133.91, 132.00, 131.43, 131.35, 131.31, 131.26, 131.16, 131.04, 129.98, 128.91, 128.84, 128.65, 128.47, 128.29, 127.99, 127.70, 127.33, 126.99, 126.95, 126.78, 126.73, 126.60, 123.15, 117.70, 109.04. APCI-MS: m/z $[M+H]^+$ calcd for $C_{55}H_{37}N_4$: 753.3018, found = 753.3009.

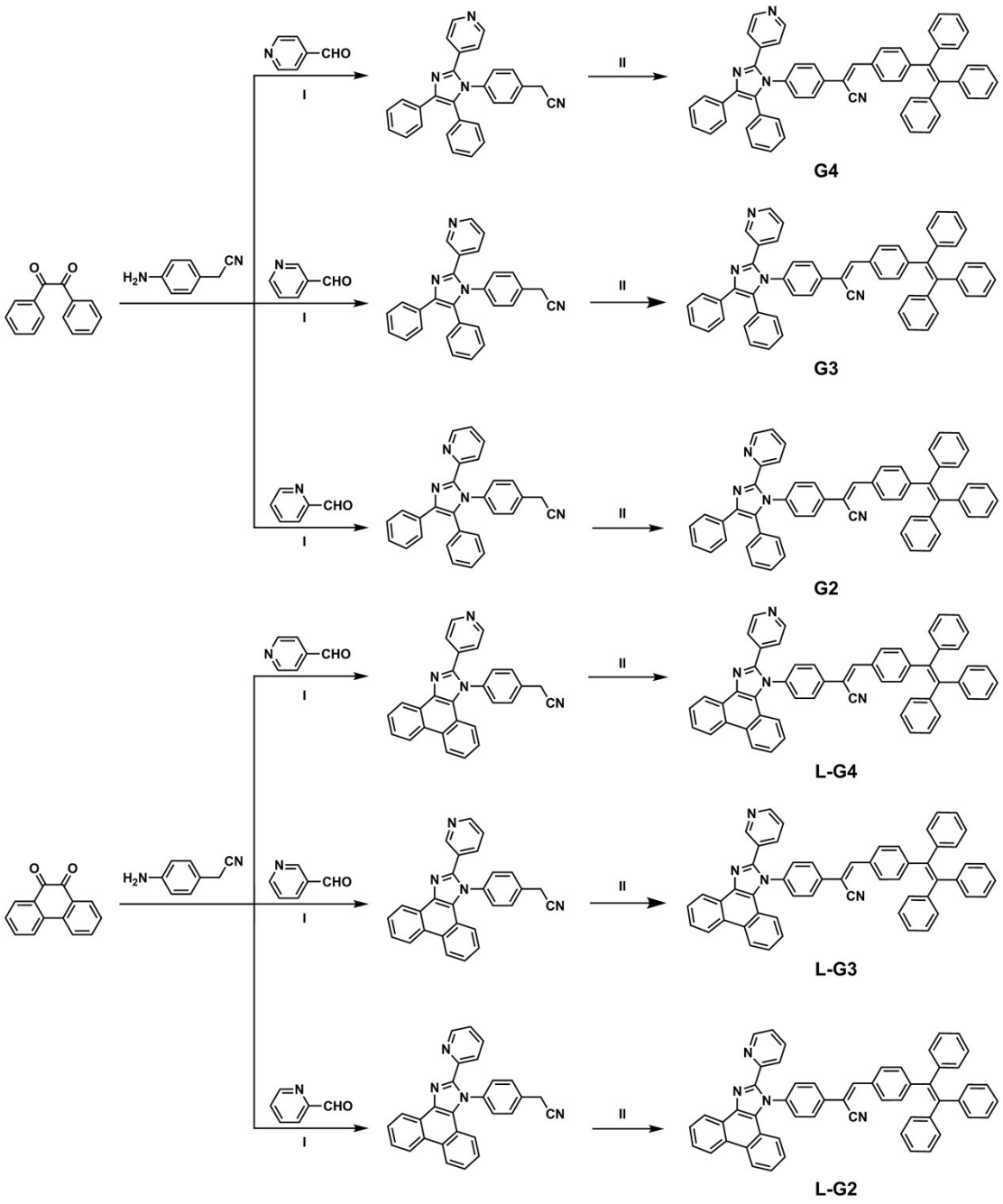

Scheme S1. Synthetic route of compounds **G4**, **G3**, **G2**, **L-G4**, **L-G3**, **L-G2**. (I) acetic acid and ammonium acetate, 12 h, 120 °C; (II) 4-(1,2,2-triphenylvinyl)benzaldehyde, t-BuOK and ethanol, 5 h, 80 °C.

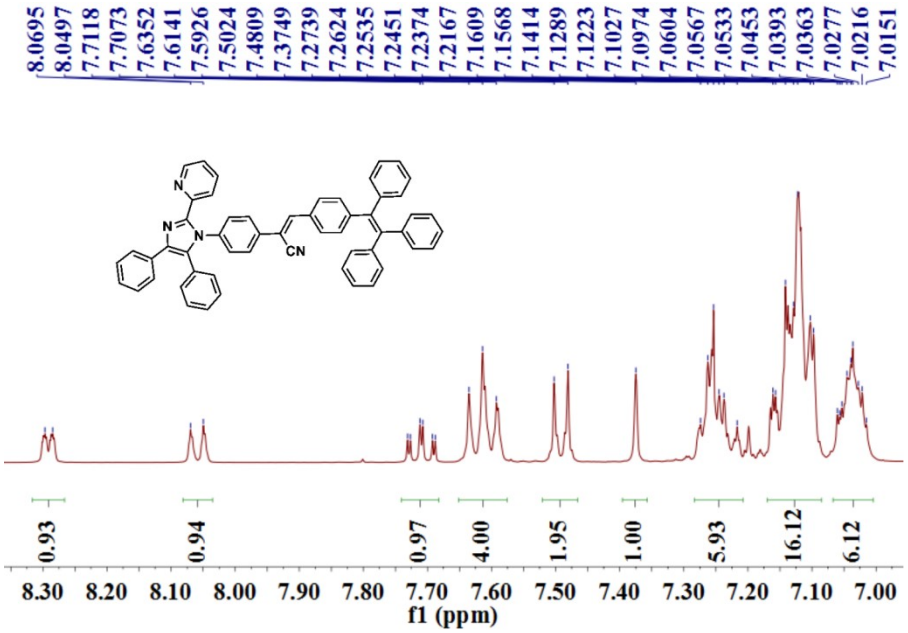

Fig. S1 The ^{1}H NMR spectrum of compound G2.

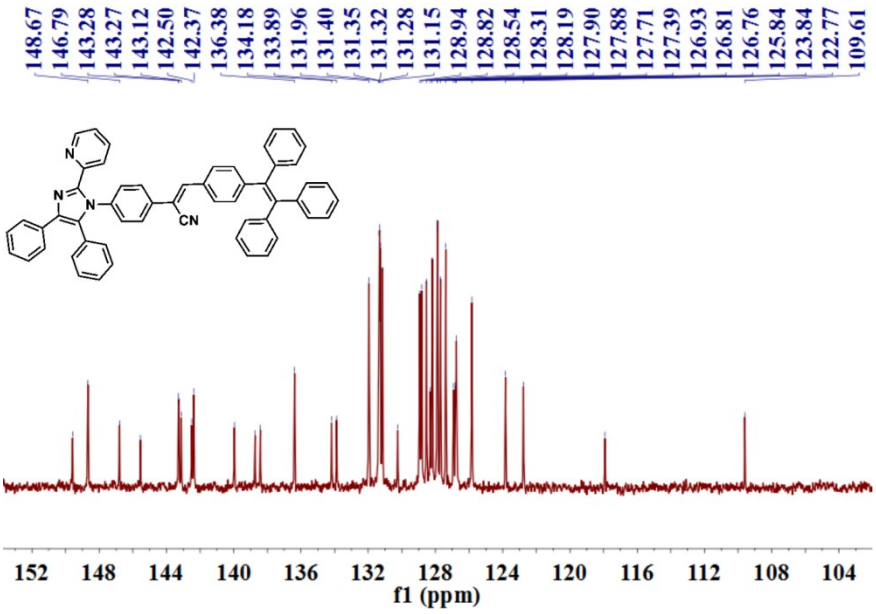

Fig. S2 The ^{13}C NMR spectrum of compound G2.

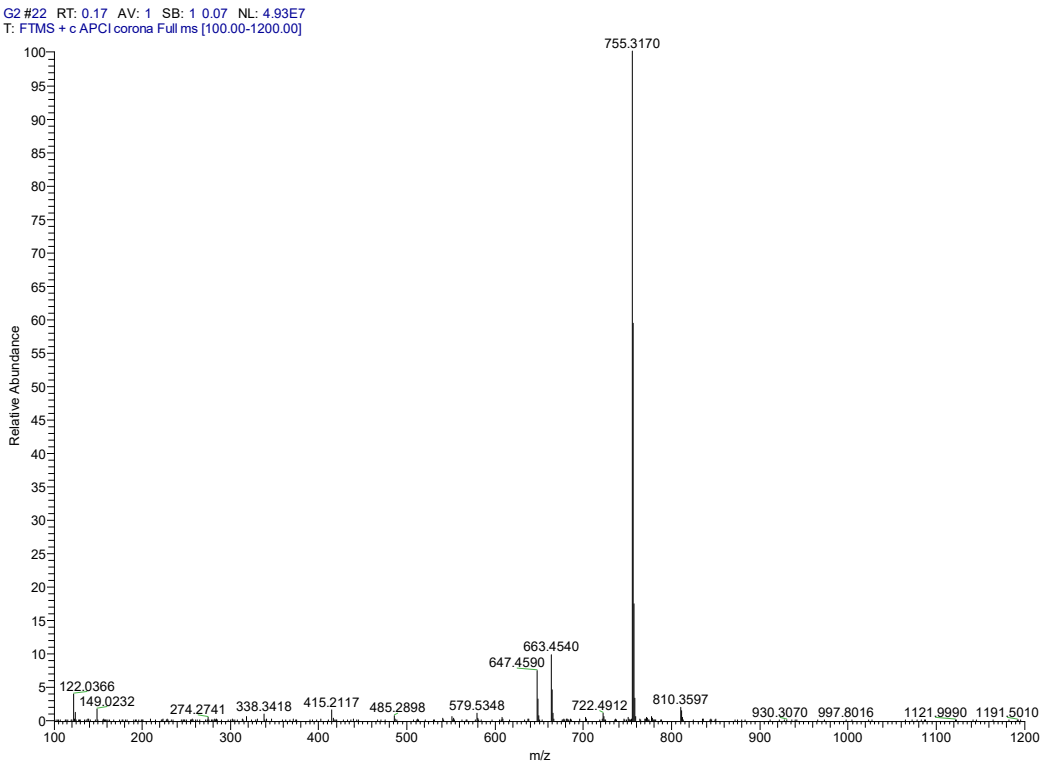

Fig. S3 The MS spectrum of compound G2.

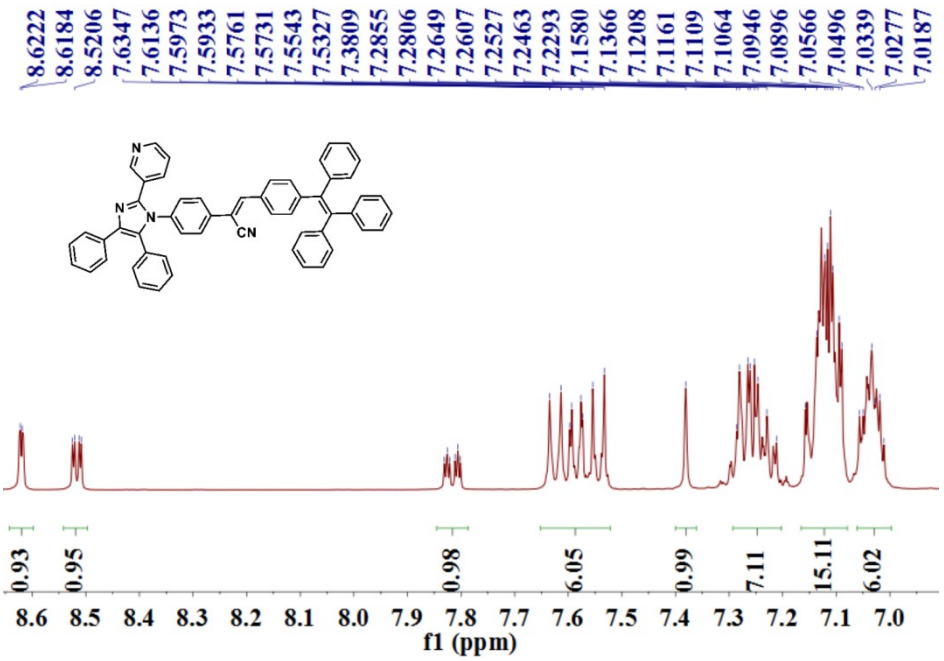

Fig. S4 The ^{1}H NMR spectrum of compound G3.

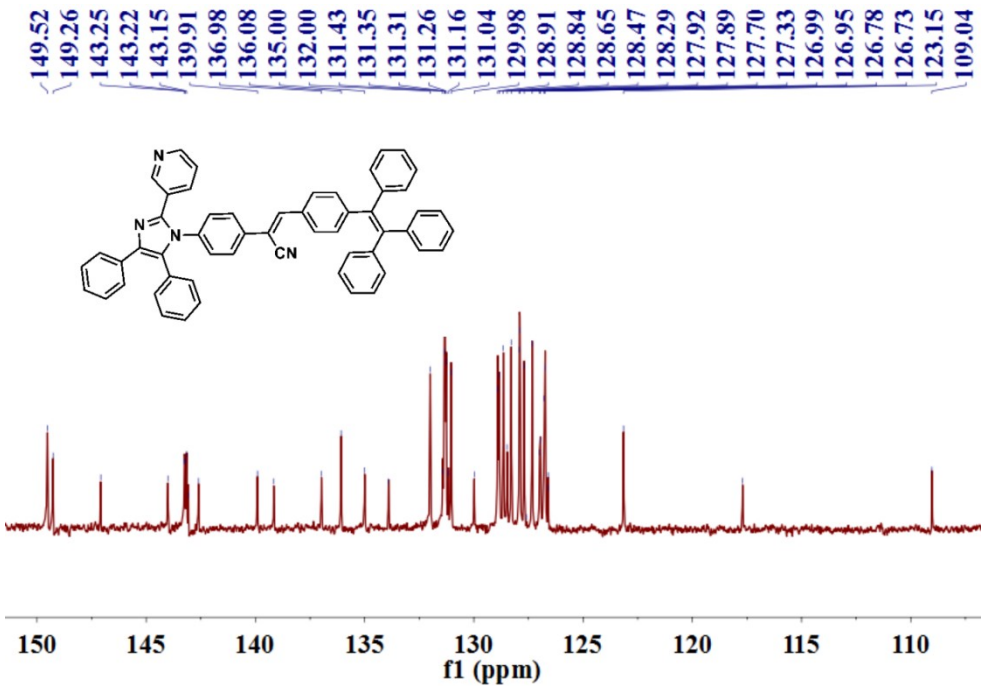

Fig. S5 The ^{13}C NMR spectrum of compound G3.

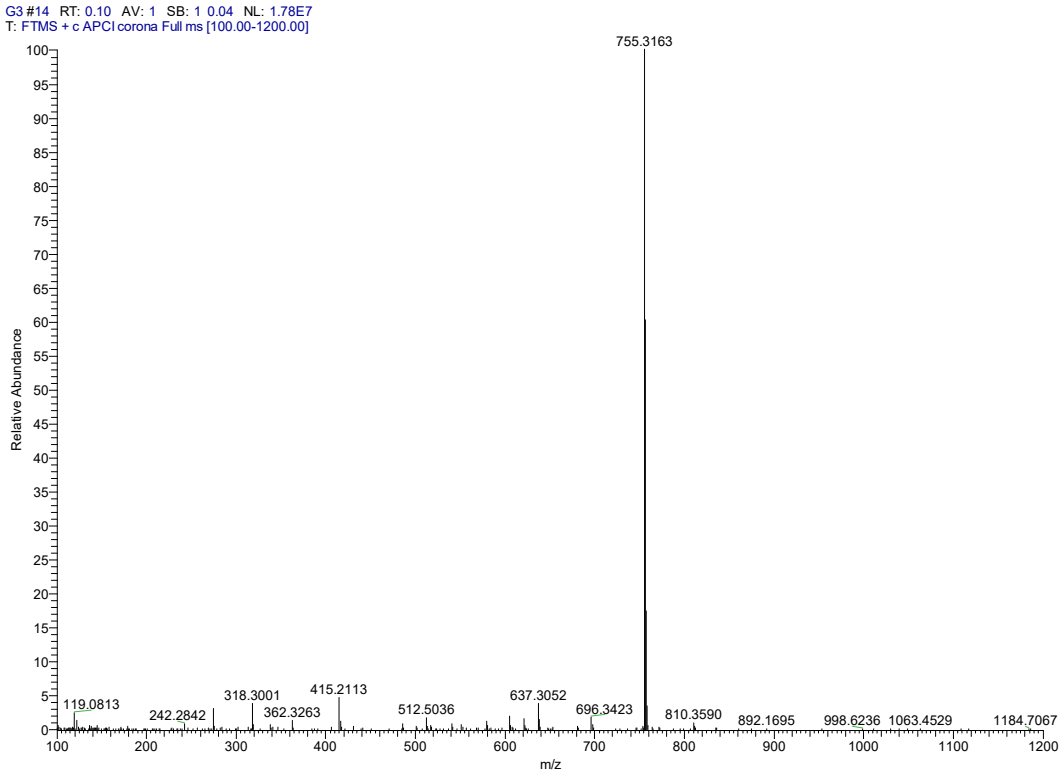

Fig. S6 The MS spectrum of compound G3.

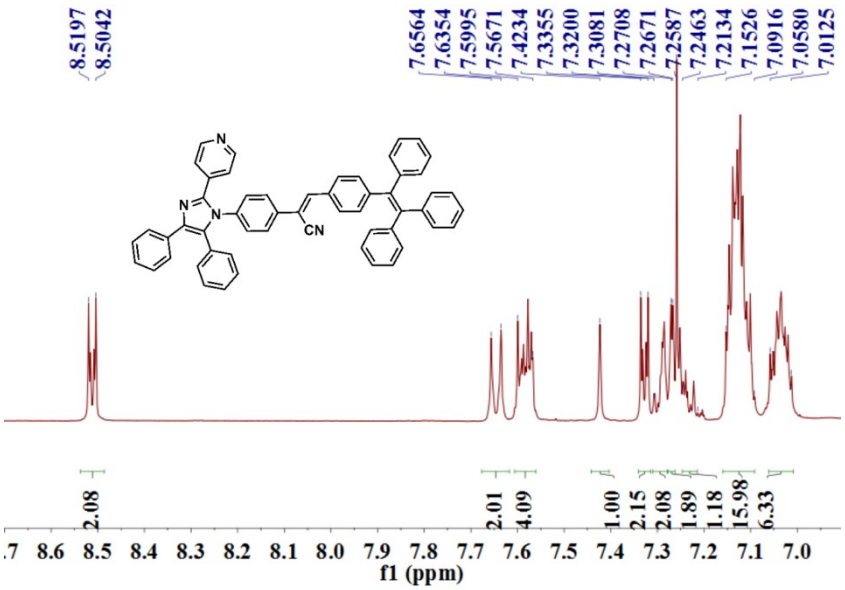

Fig. S7 The ^{1}H NMR spectrum of compound G4.

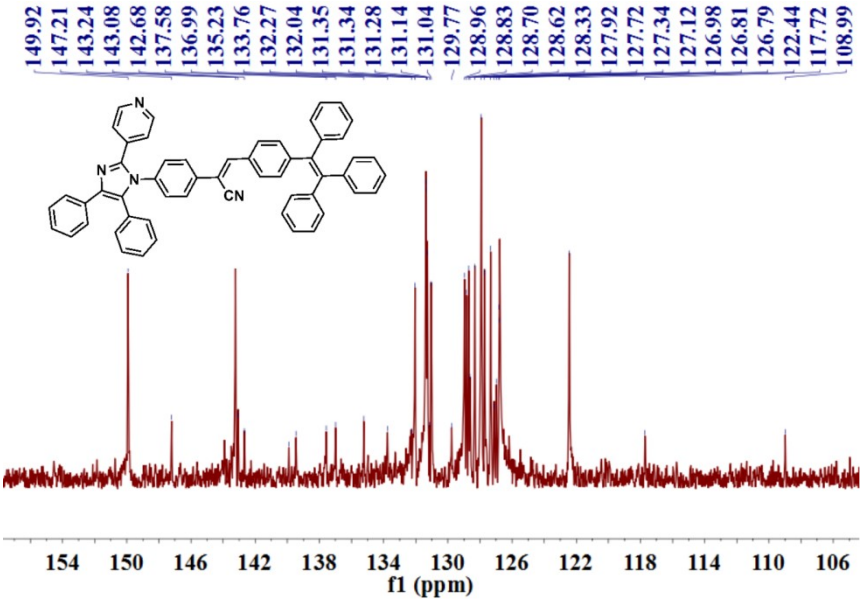

Fig. S8 The ^{13}C NMR spectrum of compound G4.

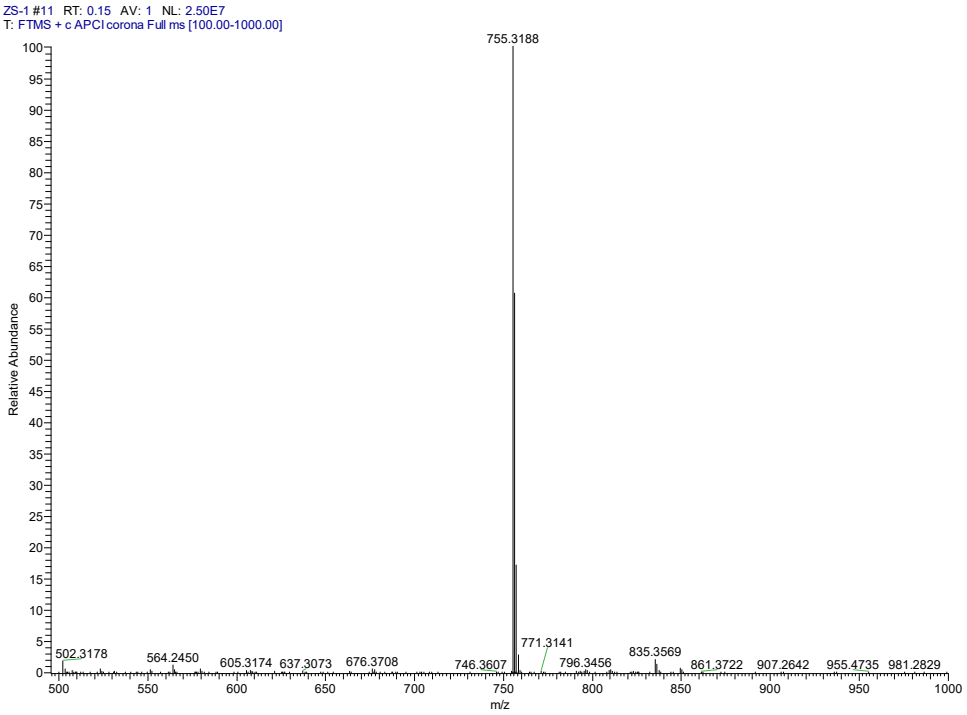

Fig. S9 The MS spectrum of compound G4.

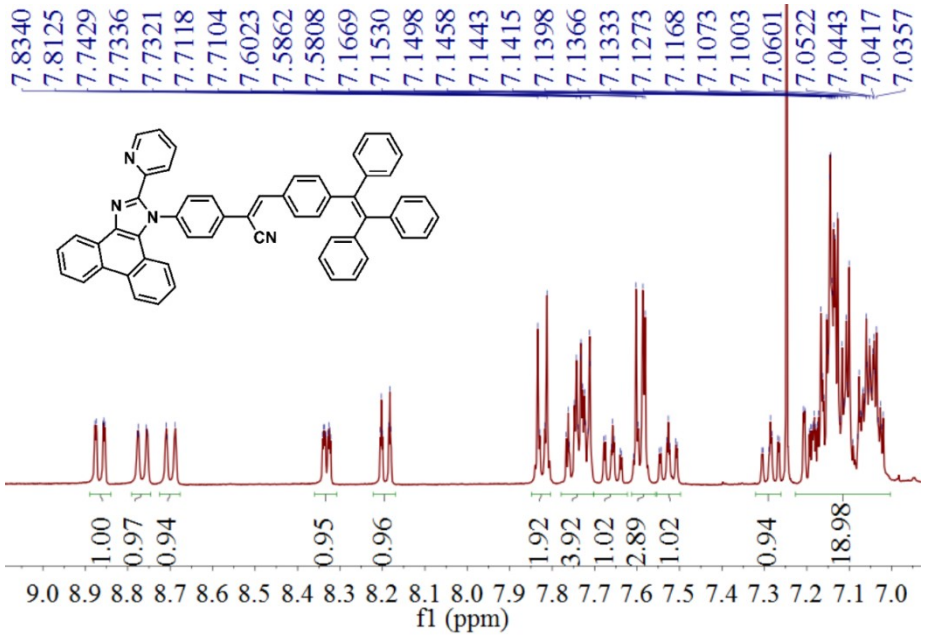

Fig. S10 The ^{1}H NMR spectrum of compound L-G2.

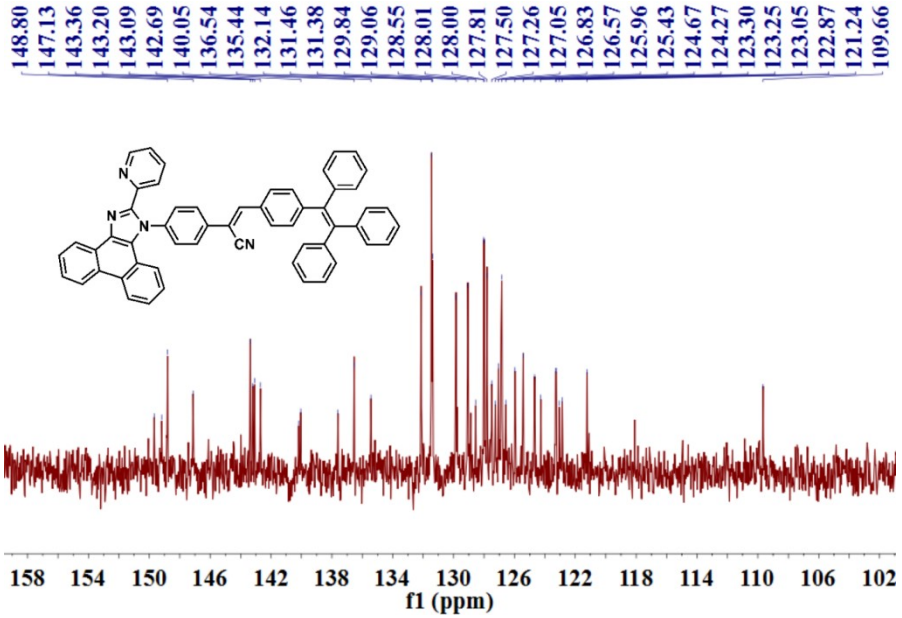

Fig. S11 The ^{13}C NMR spectrum of compound G4.

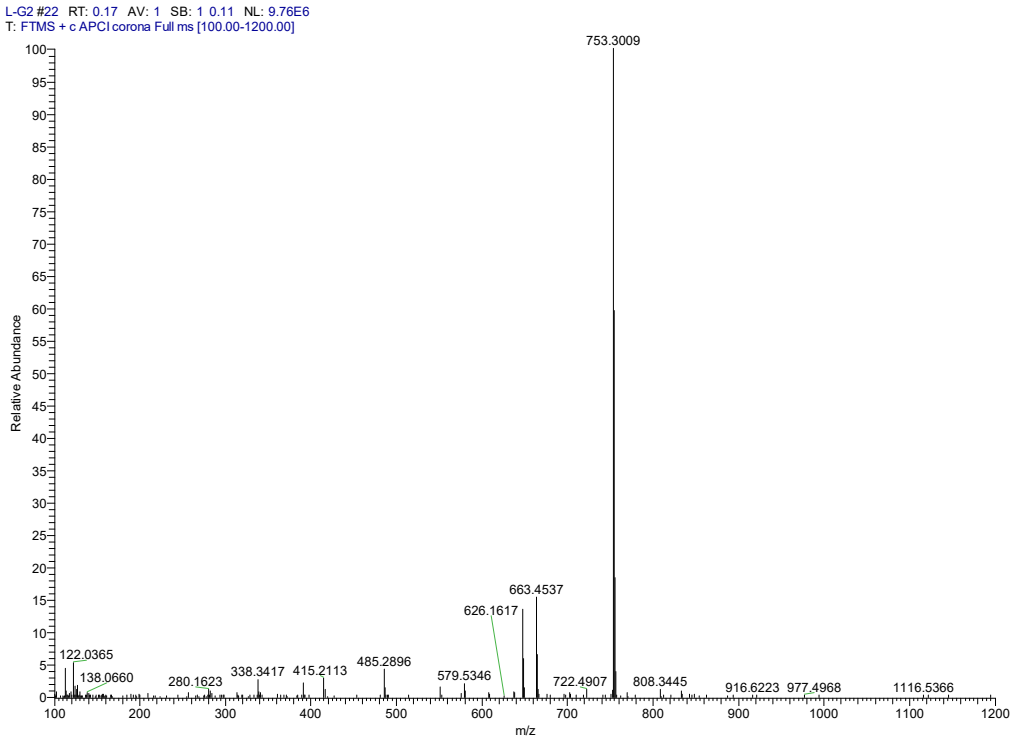

Fig. S12 The MS spectrum of compound L-G2.

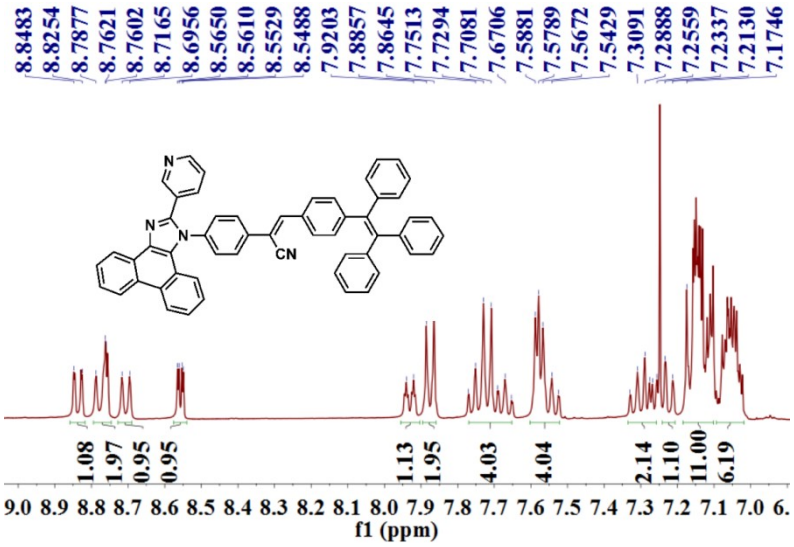

Fig. S13 The ^{1}H NMR spectrum of compound L-G3.

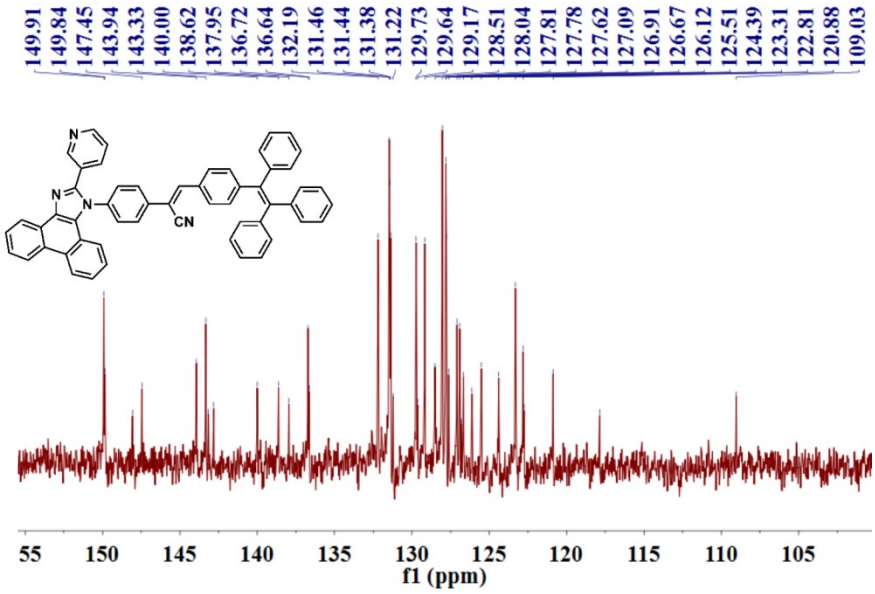

Fig. S14 The ^{13}C NMR spectrum of compound L-G3.

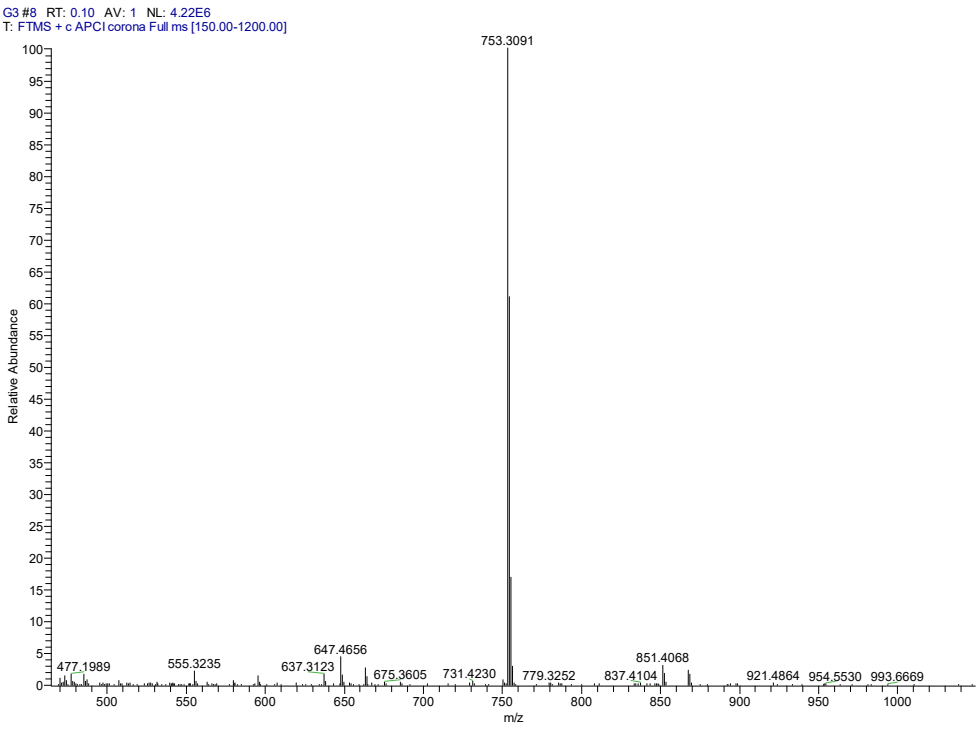

Fig. S15 The MS spectrum of compound L-G3.

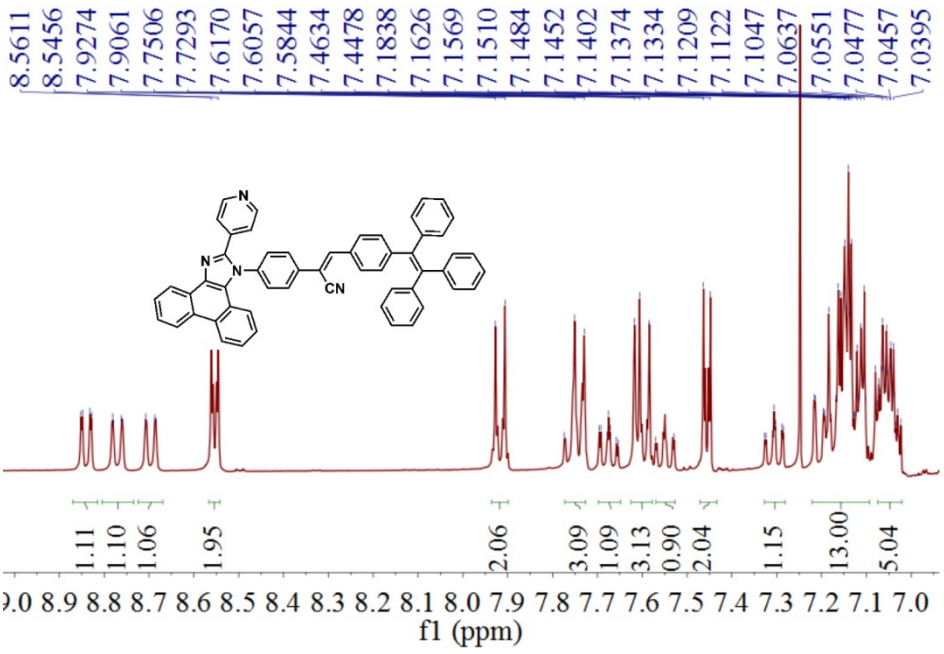

Fig. S16 The ^{1}H NMR spectrum of compound L-G4.

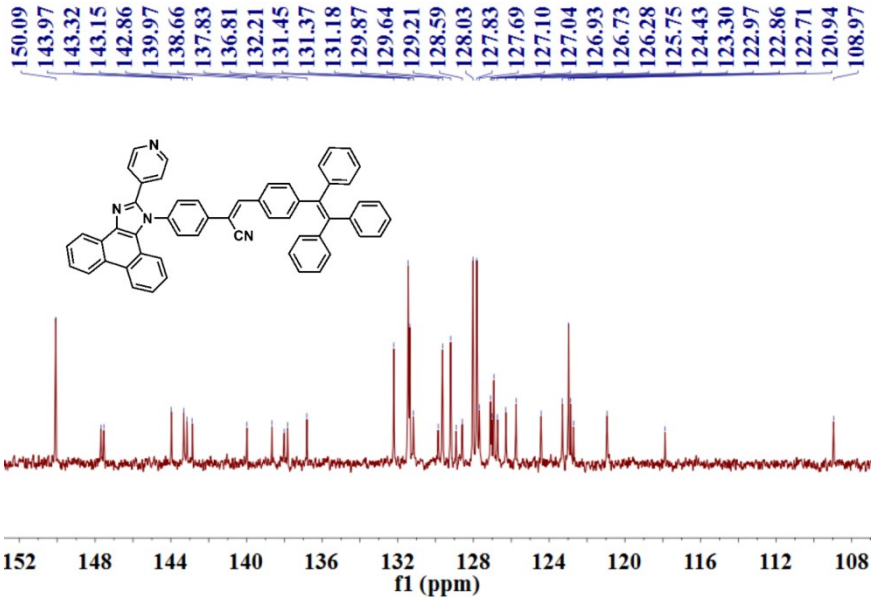

Fig. S17 The ^{13}C NMR spectrum of compound L-G4.

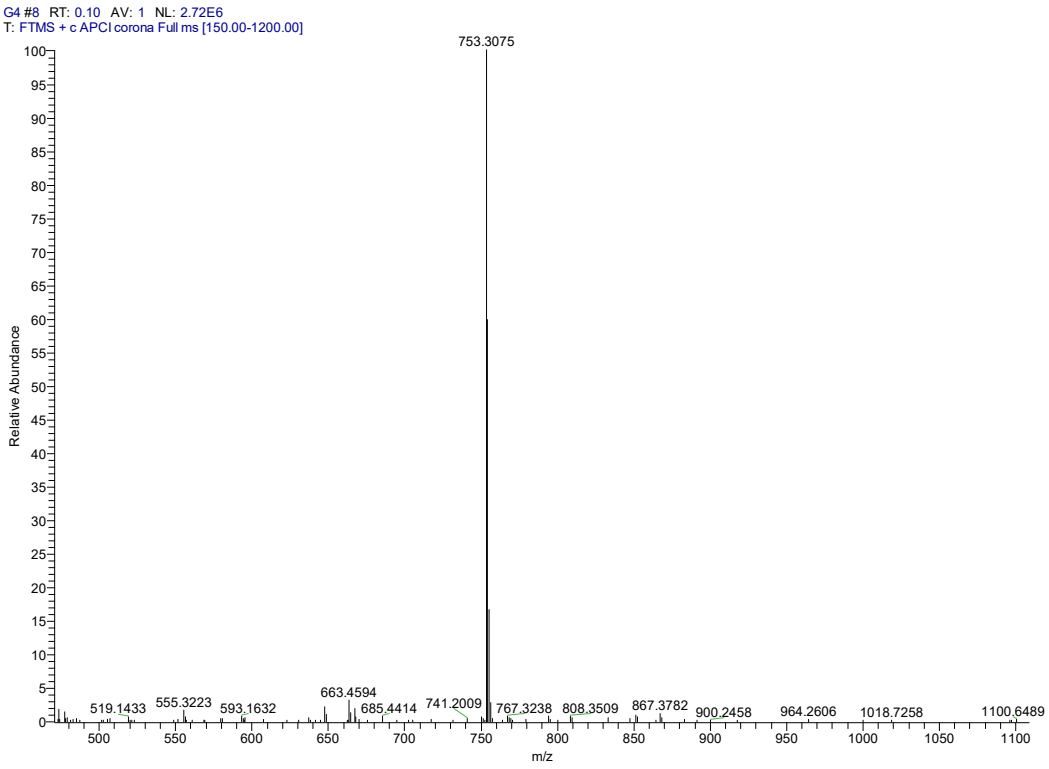

Fig. S18 The MS spectrum of compound L-G4.

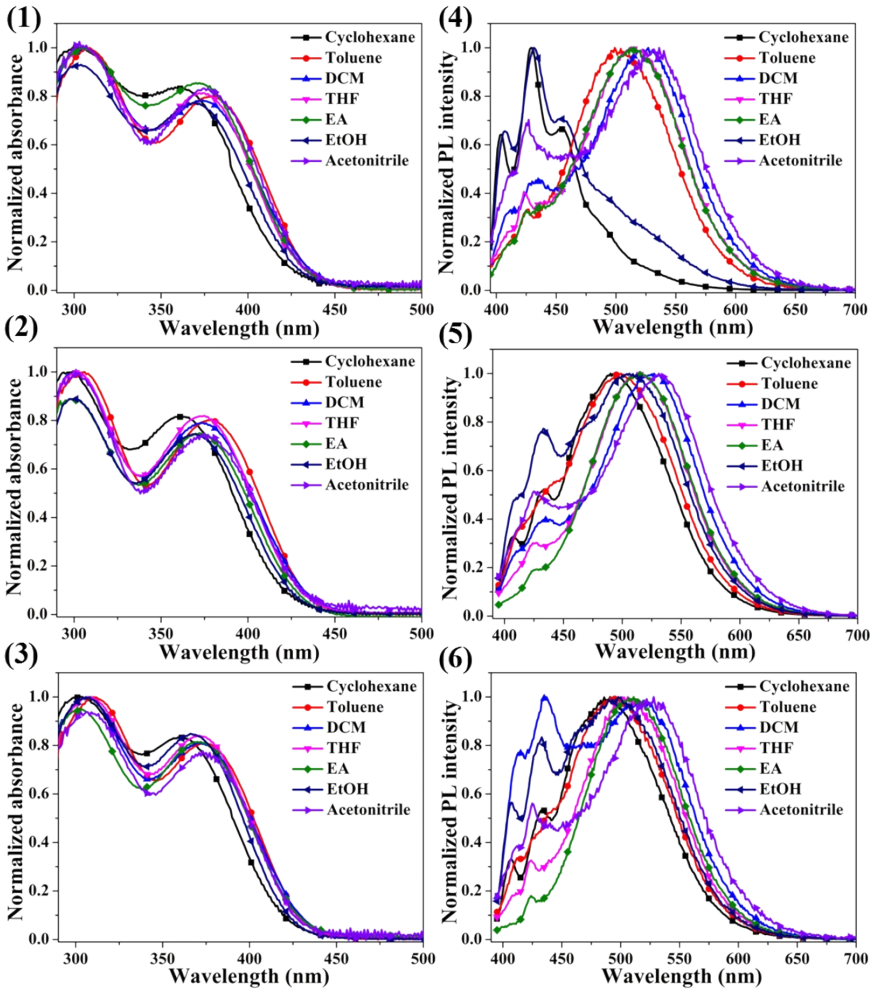

Fig. S19 The normalized absorption and PL intensity spectra of **G4** (1, 4), **G3**(2, 5), **G2** (3, 6) in the different solvents.

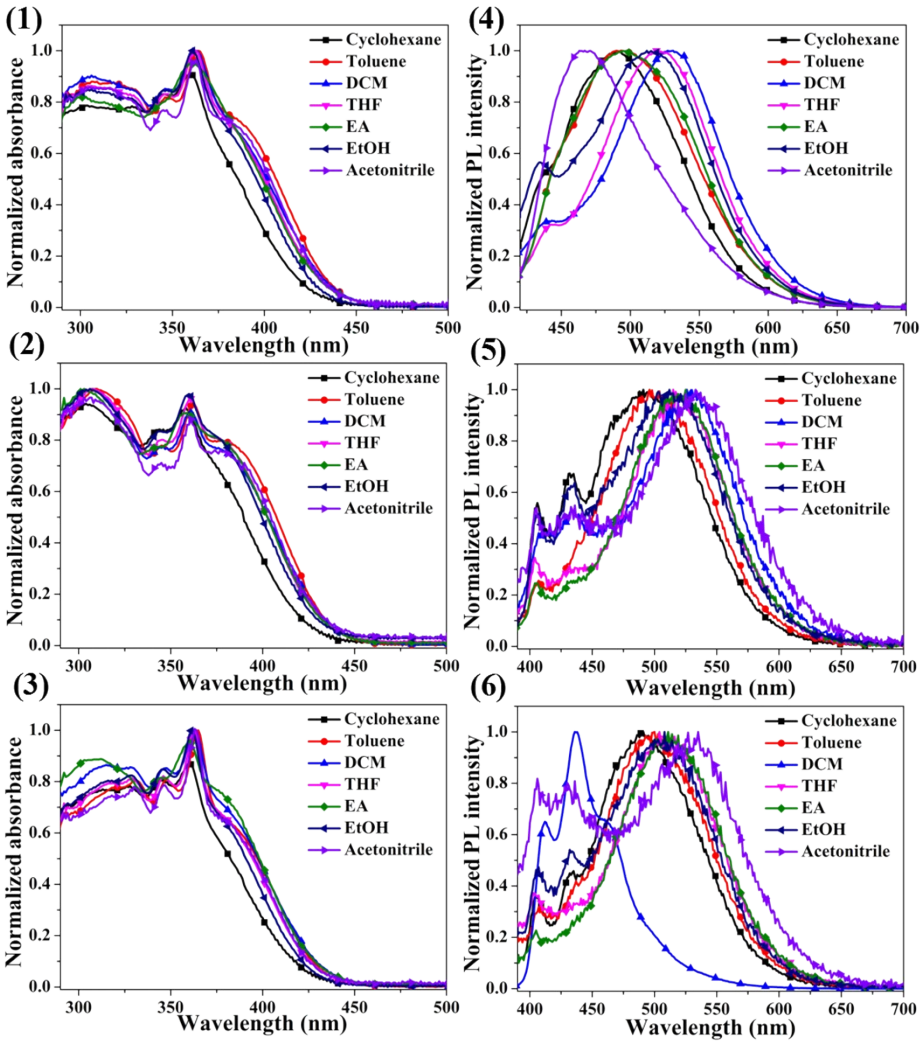

Fig. S20 The normalized absorption and PL intensity spectra of **L-G4** (1, 4), **L-G3**(2, 5), **L-G2** (3, 6) in the different solvents.

Table S1. Optical data of the compounds in different solvents and in the solid state

Compds	solvents	λ_{ab}[a] (nm)	λ_{em}[b] (nm)	$\Delta\nu$ [c] (cm^{-1})	Compds	solvents	λ_{ab}[a] (nm)	λ_{em}[b] (nm)	$\Delta\nu$ [c] (cm^{-1})
	Cyclohexane	360	429	4468		Cyclohexane	360	490	7370
	Toluene	379	499	6345		Toluene	364	490	7064
	DCM	374	527	7763		DCM	362	531	8792
G4	THF	374	513	7245	**L-G4**	THF	362	519	8356
	EA	372	512	7350		EA	361	498	7621
	EtOH	369	431	3898		EtOH	361	512	8170
	Acetonitrile	374	536	8021		Acetonitrile	363	467	6135
	Cyclohexane	360	490	7370		Cyclohexane	360	491	7411
	Toluene	378	499	6415		Toluene	362	496	7463
	DCM	373	527	7834		DCM	360	533	9016
G3	THF	375	517	7324	**L-G3**	THF	361	515	8283
	EA	372	517	7539		EA	359	525	8808
	EtOH	369	508	7415		EtOH	360	512	8247
	Acetonitrile	374	531	7906		Acetonitrile	360	533	9016
	Cyclohexane	357	491	7645		Cyclohexane	360	491	7411
	Toluene	374	494	6495		Toluene	362	500	7624
	DCM	372	513	7389		DCM	360	436	4842
G2	THF	373	506	7047	**L-G2**	THF	361	504	7860
	EA	372	511	7312		EA	359	511	8236
	EtOH	368	498	7094		EtOH	360	508	8093
	Acetonitrile	373	528	7870		Acetonitrile	361	535	9009

[a] Peak position of the maximum absorption band. [b] Peak position of fluorescence emission, excited at the absorption maximum. [c] Stokes' shift in cm^{-1}. [d,e] absolute fluorescence quantum yields (Φ_{PL}) and wavelength (λ_{PL}) before and after grinding in the solid state.

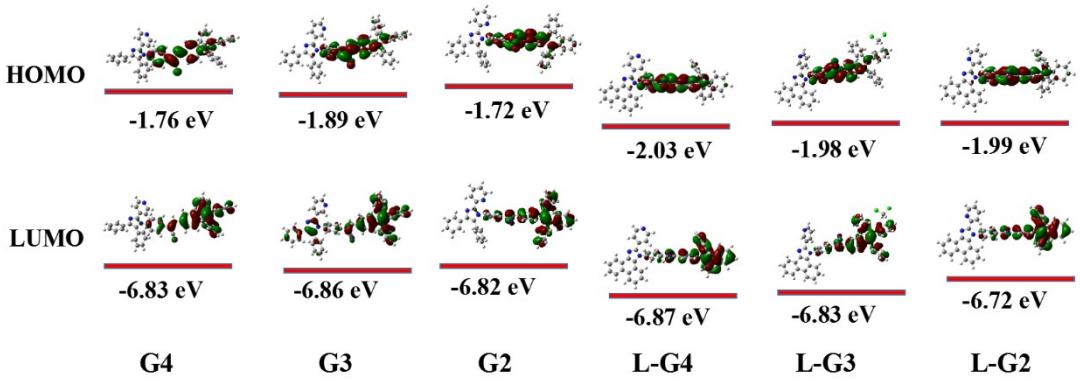

Fig. S21 The HOMO and LUMO electron cloud distribution of the compounds.

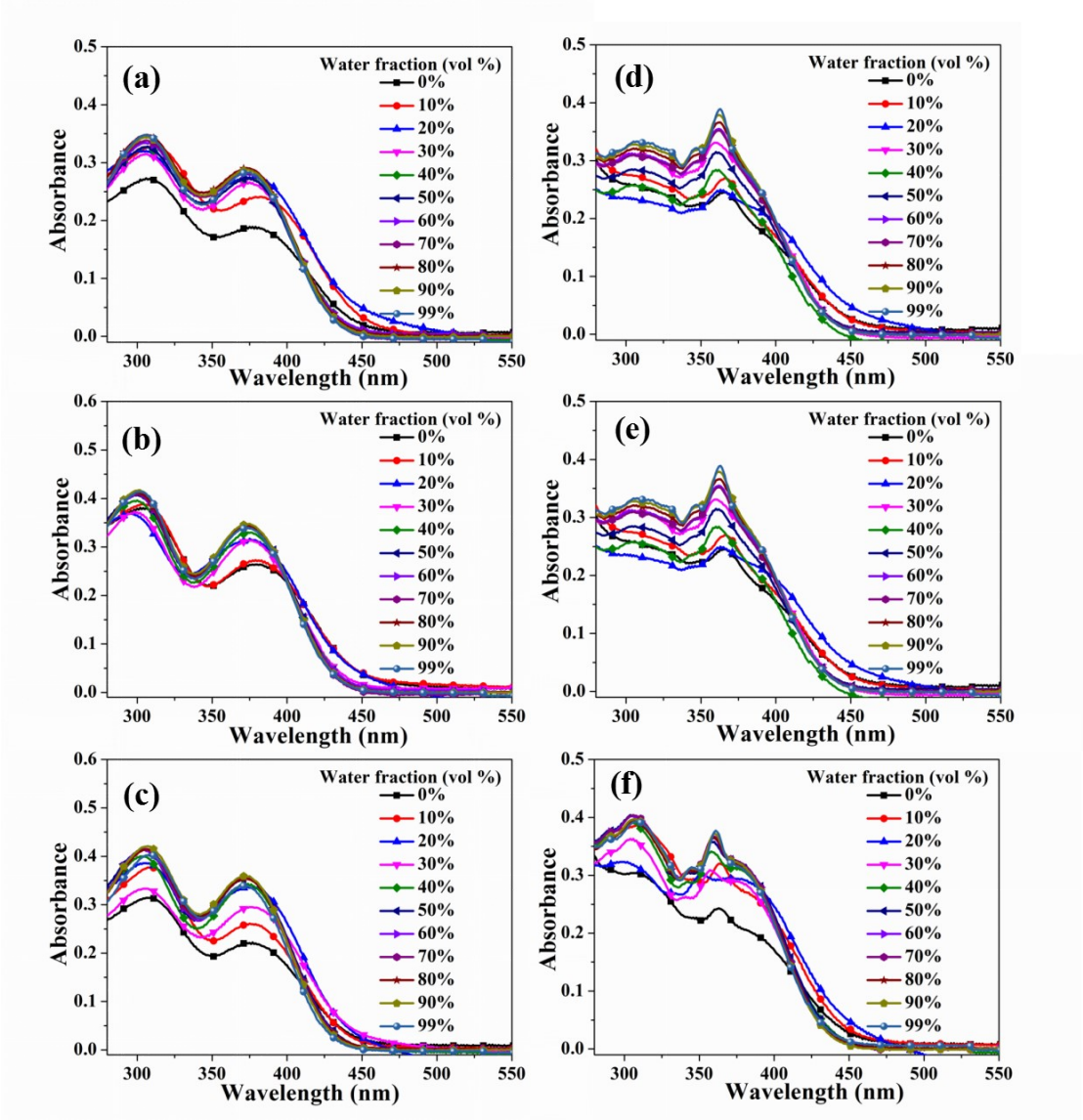

Fig. S22 (a) The UV-vis absorption spectra of compounds **G4** (a), **G3** (b), **G2** (c), **L-G4** (d), **L-G3** (e), **L-G2** (f) in THF/H_2O mixtures with different water volume fractions.

Table S2. Fluorescence quantum yield data of the compounds

Cpds	Φ (0% H_2O)	Φ (99% H_2O)	Φ (solid)	Cpds	Φ (0% H_2O)	Φ (99% H_2O)	Φ (solid)
G2	0.45	26.57	67	**L-G2**	0.77	45.57	48
G3	0.48	29.99	72	**L-G3**	0.27	39.20	52
G4	0.47	31.85	67	**L-G4**	0.45	35.16	40

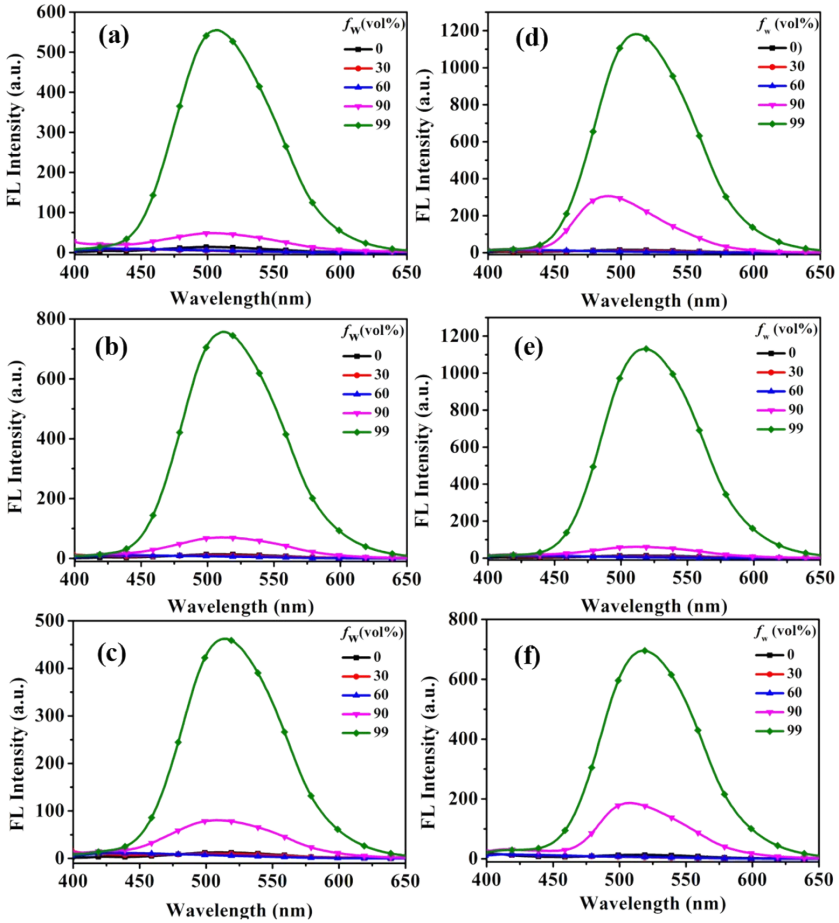

Fig. S23 (a) The FL spectra of compounds **G2** (a), **G3** (b), **G4** (c), **L-G2** (d), **L-G3** (e), **L-G4** (f) in glycerinum/H_2O mixtures with different water volume fractions.

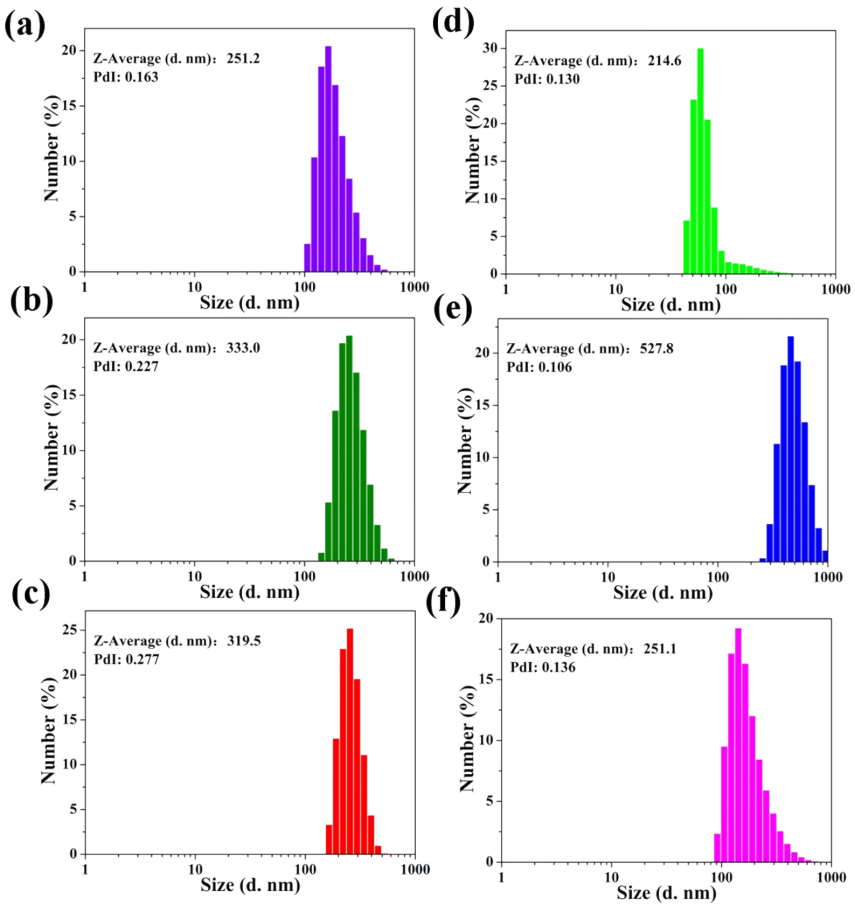

Fig. S24 DLS size distribution of of the nanoparticles of **G4** (a), **G3** (b), **G2** (c), **L-G4** (d), **L-G3** (e), **L-G2** (f) in THF/H_2O solution (1 : 9, v/v).

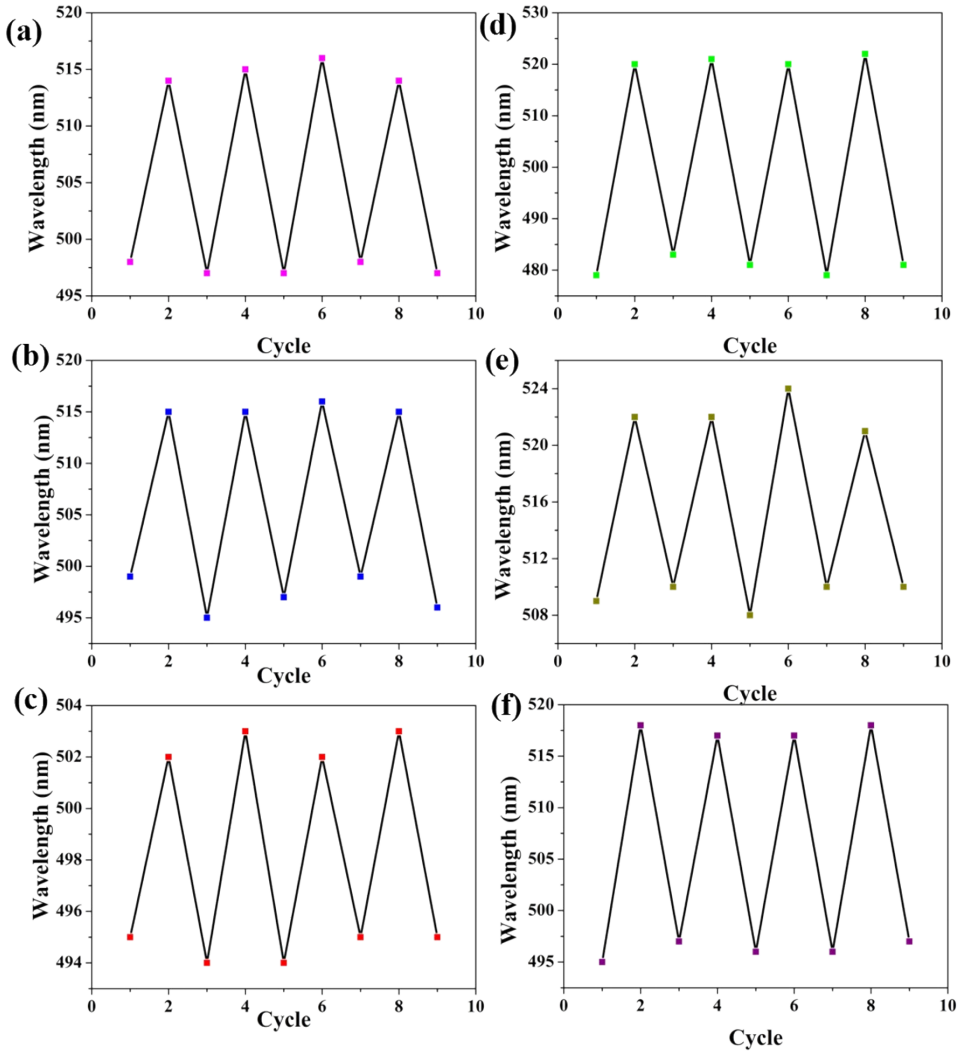

Fig. S25 Repeated switching of compounds **G4** (a), **G3** (b), **G2** (c), **L-G4** (d), **L-G3** (e), **L-G2** (f) by ground-heated cycles.

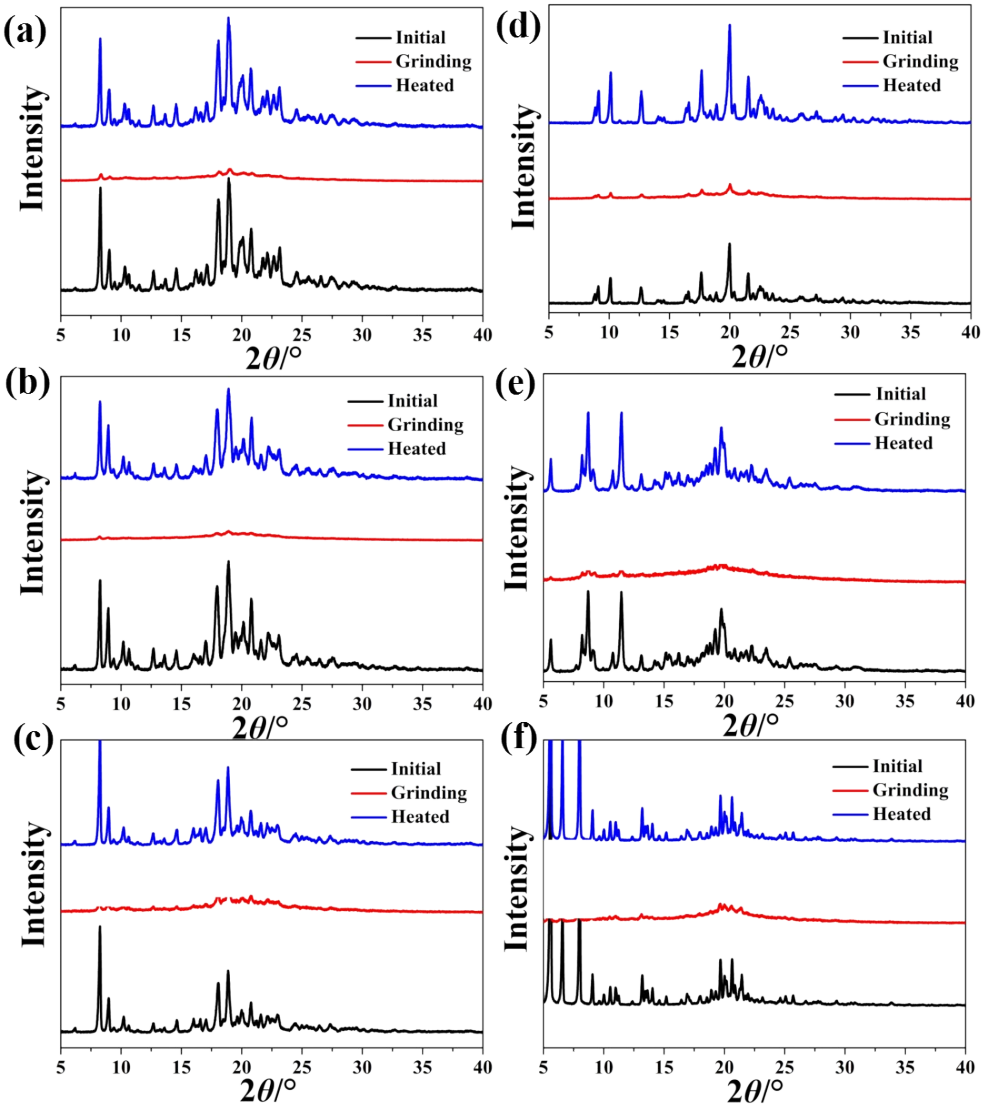

Fig. S26 PXRD patterns of pristine, ground and fumed with EtOH samples of **G4** (a), **G3** (b), **G2** (c), **L-G4** (d), **L-G3** (e), **L-G2** (f).

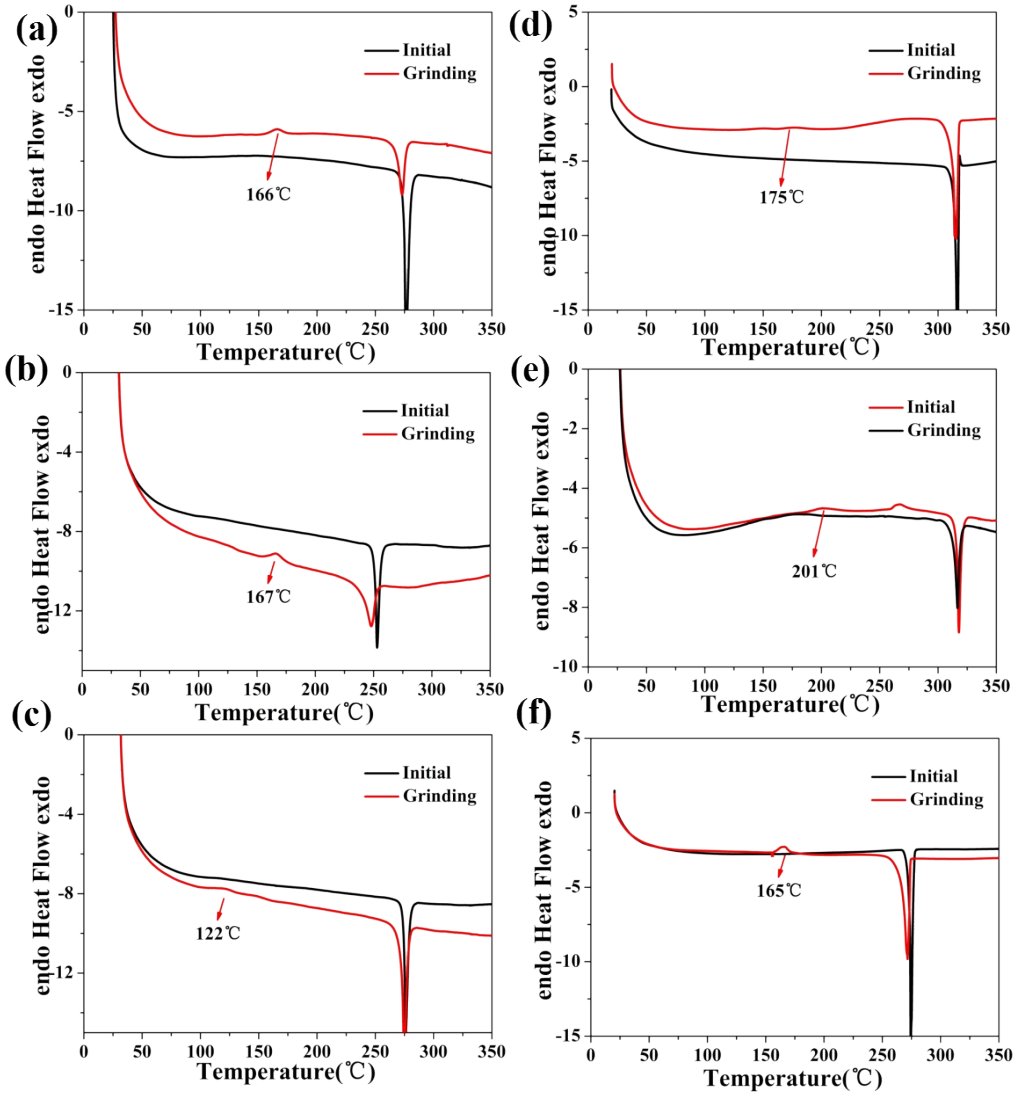

Fig. S27 DSC curve of **G4** (a), **G3** (b), **G2** (c), **L-G4** (d), **L-G3** (e), **L-G2** (f) in the pristine and ground powders. (Scan rate: 10 °C/min)

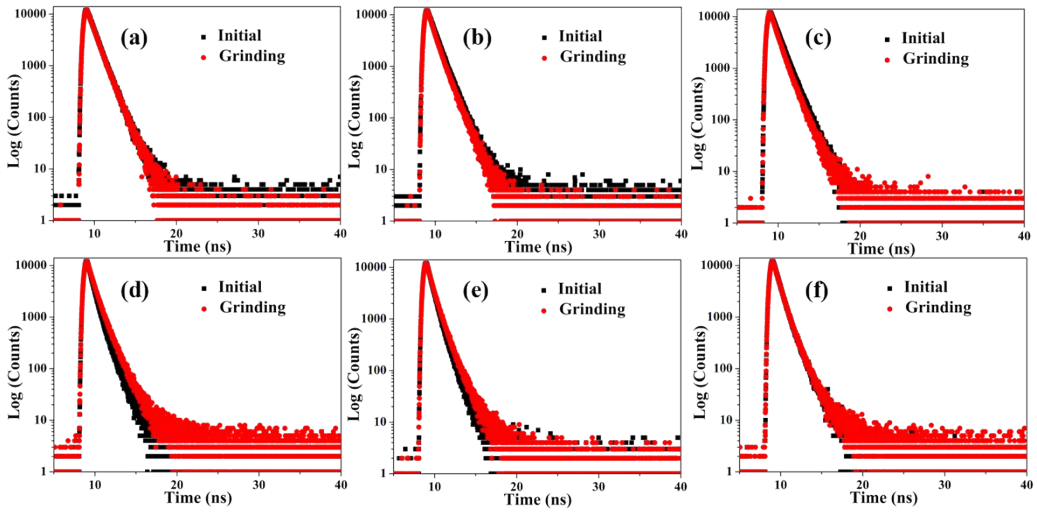

Fig. S28 The fluorescence lifetimes of **G2** (a), **G3** (b), **G4** (c), **L-G2** (d), **L-G3** (e), **L-G4** (f) in the pristine and ground powders.

Table S3 Summary of crystallographic data and structure refinement details for **G3** and **L-G3**

Compounds	**L-G3**	**G3**
Formula	$C_{55}H_{36}N_4$	$C_{55}H_{38}N_4$
Mr	752.29	754.89
Temperature	293	293
Crystal system	Triclinic	Monoclinic
Space group	*P*-1	$P2_1/c$
a (Å)	12.057	42.8295
b (Å)	12.616	9.8166
c (Å)	16.803	19.5245
Volume	2160.5	8171.0
Z, Calculated density	2, 1.288 (g/cm^{-3})	8, 1.227 (g/cm^{-3})
F(000)	872.0	3168.0
Data/restraints/parameters	7631/0/559	13930/134/1098
Goodness-of-fit on F^2	1.061	0.950
Largest diff.peak and hole	0.88 and -0.49 $e.A^{-3}$	0.33 and -0.51 $e.A^{-3}$
Limiting indices	$-14 \le h \le 11$ $-14 \le k \le 14$ $-20 \le l \le 15$	$-50 \le h \le 31$ $-7 \le k \le 11$ $-20 \le l \le 23$
Reflection collected / unique	7631 [R_{int} = 0.0193, R_{sigma} = 0.0190]	13930 [R_{int} = 0.0751, R_{sigma} = 0.1045]
Final R indices [$I>2\sigma(I)$]	R_1 = 0.0483, wR_2 = 0.1408	R_1 = 0.0705, wR_2 = 0.1772
R indices (all)	R_1 = 0.0509, wR_2 = 0.1451	R_1 = 0.1652, wR_2 = 0.2333

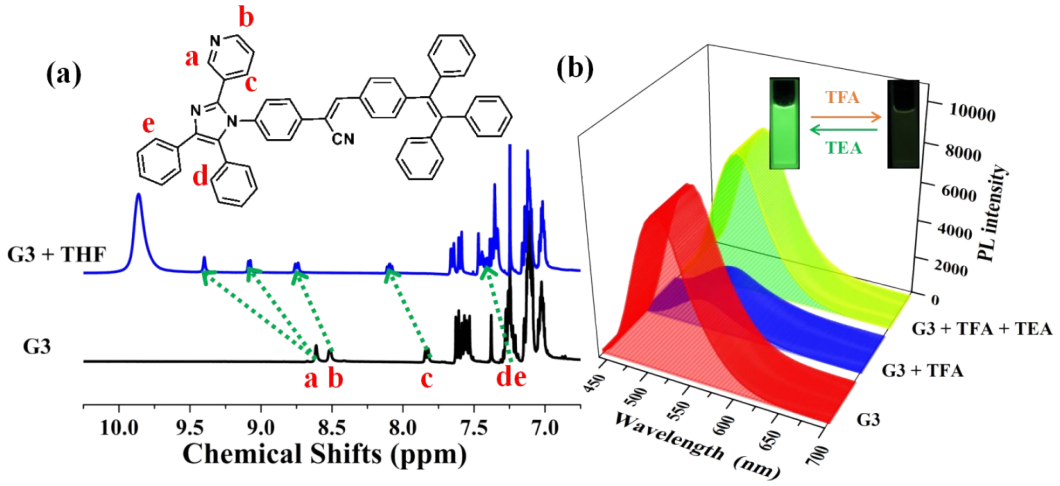

Fig. S29 (a) ^{1}H NMR spectra of G3 in $CDCl_3$ in the absence and presence of 2 equivalents TFA; (b) change in the PL spectra of G3 between off and on by reversibly treated with TFA-TEA.

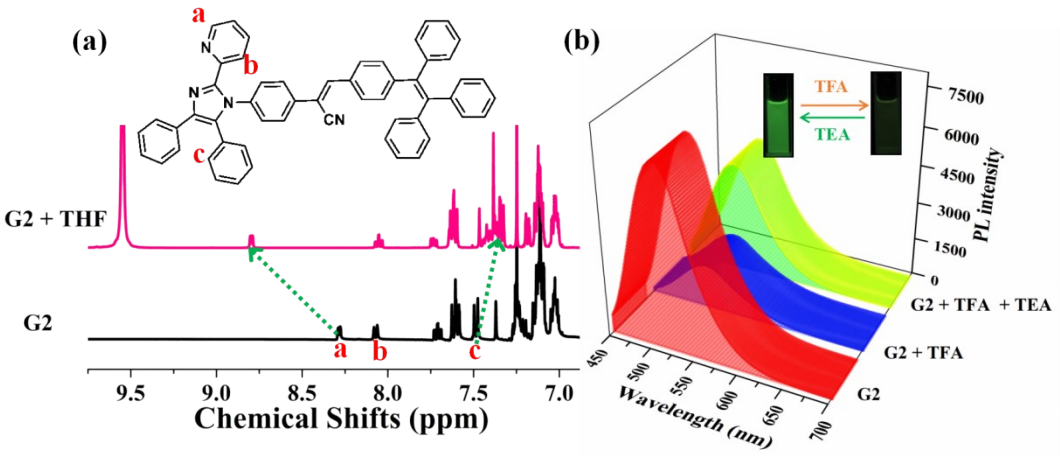

Fig. S30 (a) ^{1}H NMR spectra of G2 in $CDCl_3$ in the absence and presence of 2 equivalents TFA; (b) change in the PL spectra of G2 between off and on by reversibly treated with TFA-TEA.

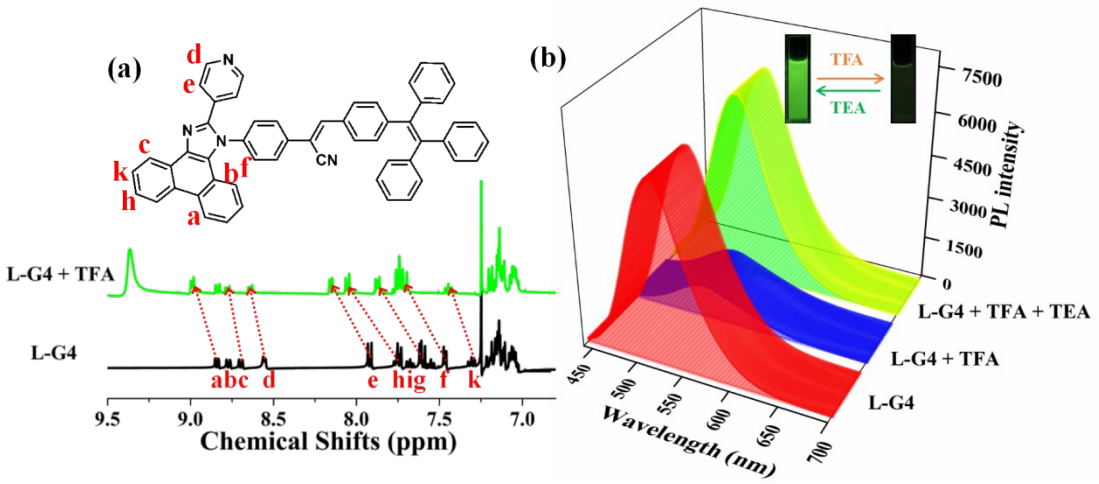

Fig. S31 ^{1}H NMR spectra of L-G4 in $CDCl_3$ in the absence and presence of 2 equivalents TFA; (b) change in the PL spectra of L-G4 between off and on by reversibly treated with TFA-TEA.

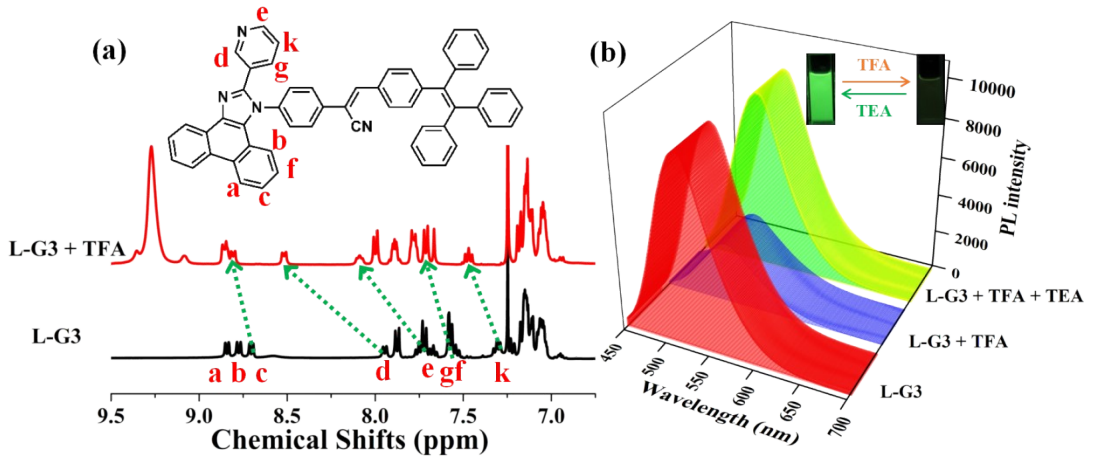

Fig. S32 (a) ^{1}H NMR spectra of L-G3 in $CDCl_3$ in the absence and presence of 2 equivalents TFA; (b) change in the PL spectra of L-G3 between off and on by reversibly treated with TFA-TEA.

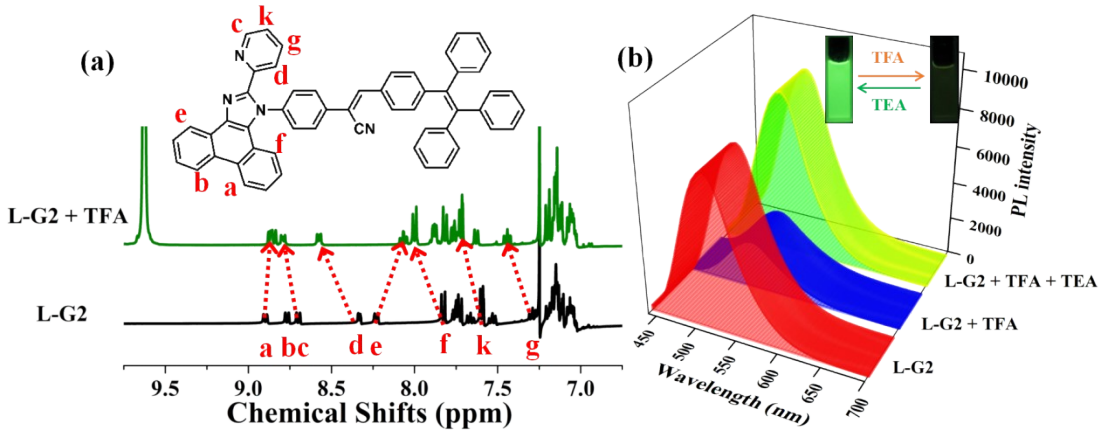

Fig. S33 (a) ^{1}H NMR spectra of L-G2 in $CDCl_3$ in the absence and presence of 2 equivalents TFA; (b) change in the PL spectra of L-G2 between off and on by reversibly treated with TFA-TEA.

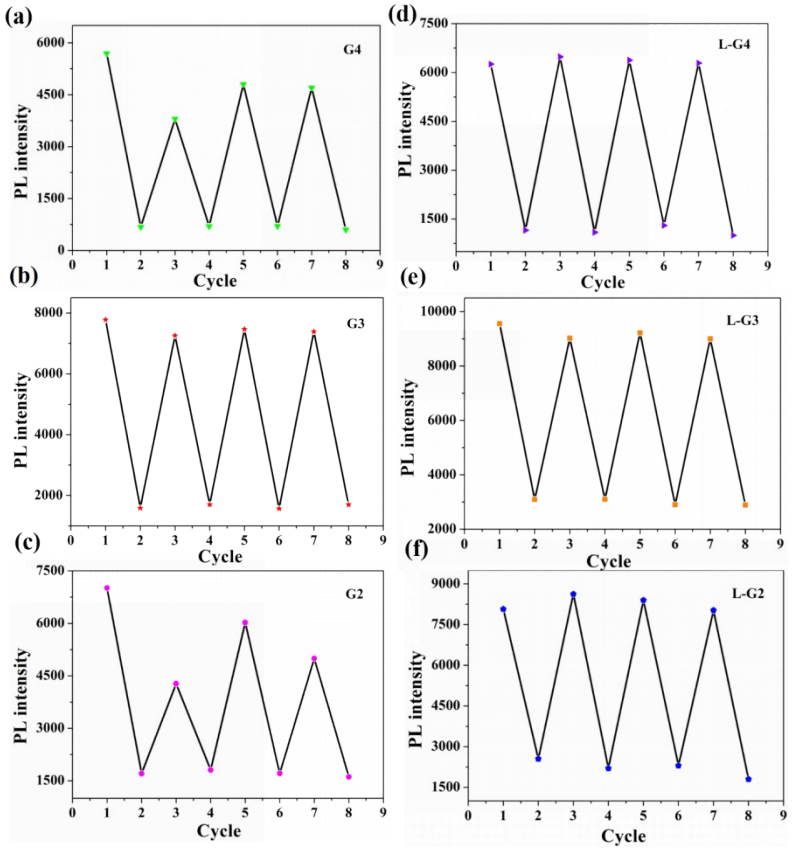

Fig. S34 Change in the emission intensity of **G4** (a), **G3** (b), **G2** (c), **L-G4** (d), **L-G3** (e), **L-G2** (f) in THF/water (v/v = 1:9) by repeated with TFA and TEA.

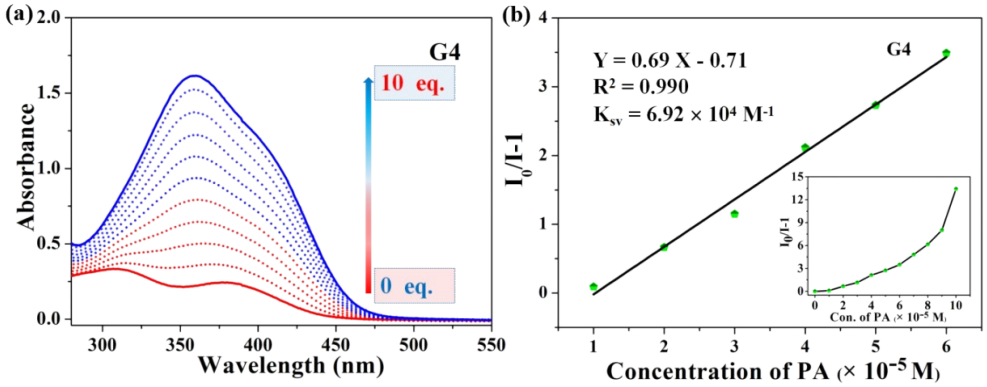

Fig. S35 (a) UV-vis spectra of **G4** upon additions of PA in THF/H_2O (v/v = 1:9) mixture. (b) Corresponding Stern-Volmer plot for lower concentration of PA detection.

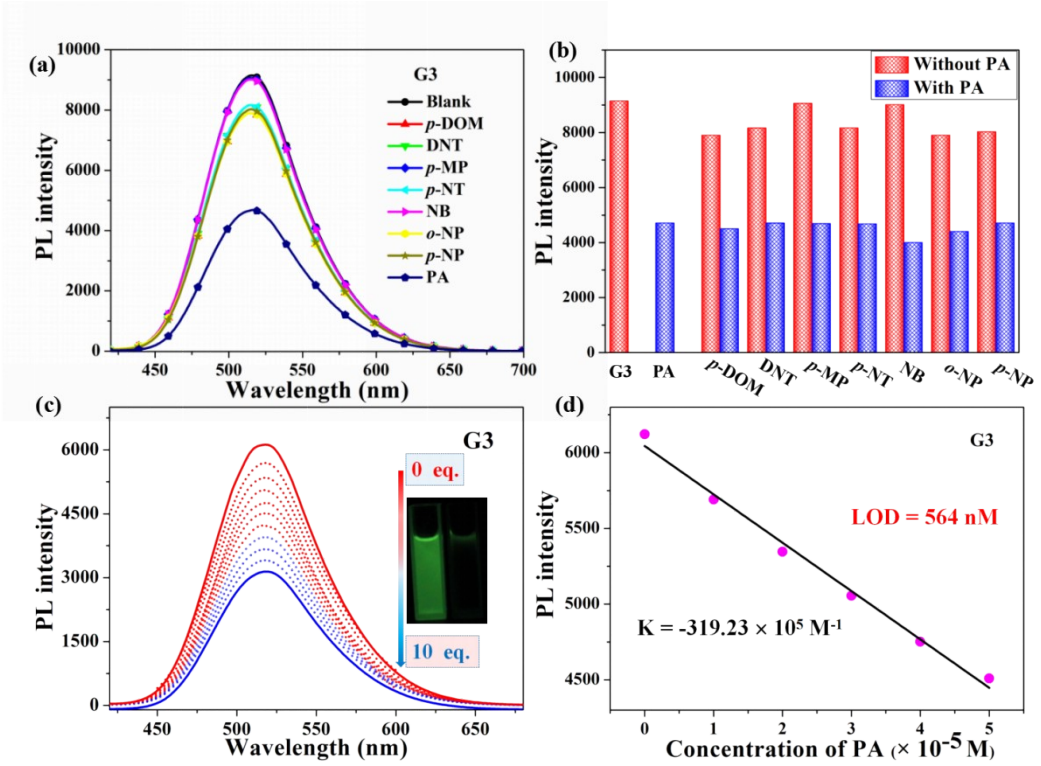

Fig. S36 (a) PL spectra response of **G3** towards different analytes (10 equiv.) in THF/water (v/v = 1 : 9) medium; (b) quenching percentages of compound **G3** (10.0 mM) with different analytes before (red) and (blue) after the addition of 10 equiv. (c) PL spectra of **G3** upn additions of PA in THF/H_2O (v/v = 1:9) mixture, Inset: photos of **G3** under UV lamp; (b) The linear relationship of **G3** between the fluorescence intensity and the PA concentration.

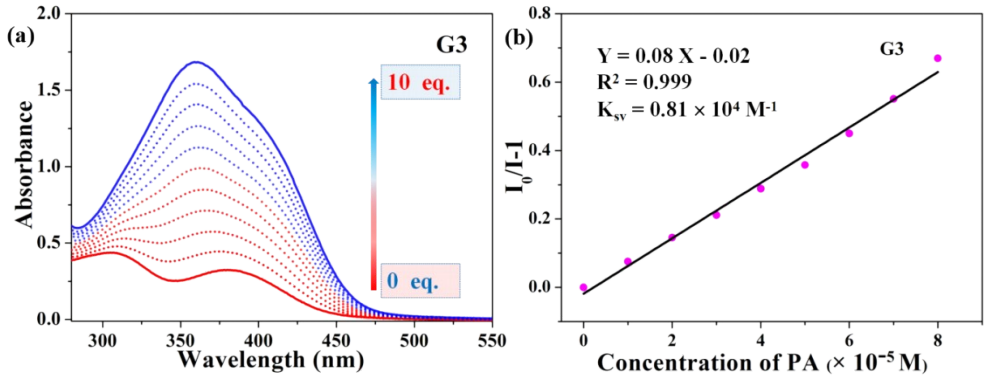

Fig. S37 (a) UV-vis spectra of **G3** upn additions of PA in THF/H_2O (v/v = 1:9) mixture. (b) Corresponding Stern-Volmer plot for lower concentration of PA detection.

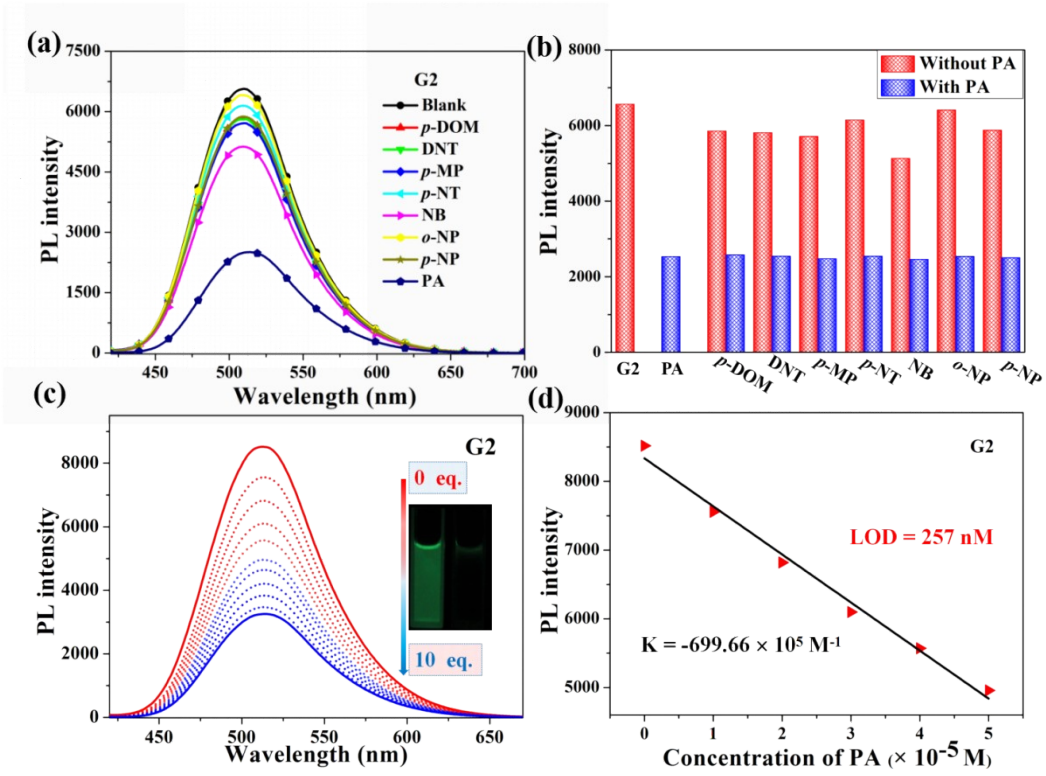

Fig. S38 (a) PL spectra response of G2 towards different analytes (10 equiv.) in THF/water (v/v = 1 : 9) medium; (b) quenching percentages of compound G2 (10.0 mM) with different analytes before (red) and (blue) after the addition of 10 equiv. (c) PL spectra of G4 upn additions of PA in THF/H_2O (v/v = 1:9) mixture, Inset: photos of G2 under UV lamp; (b) The linear relationship of G2 between the fluorescence intensity and the PA concentration.

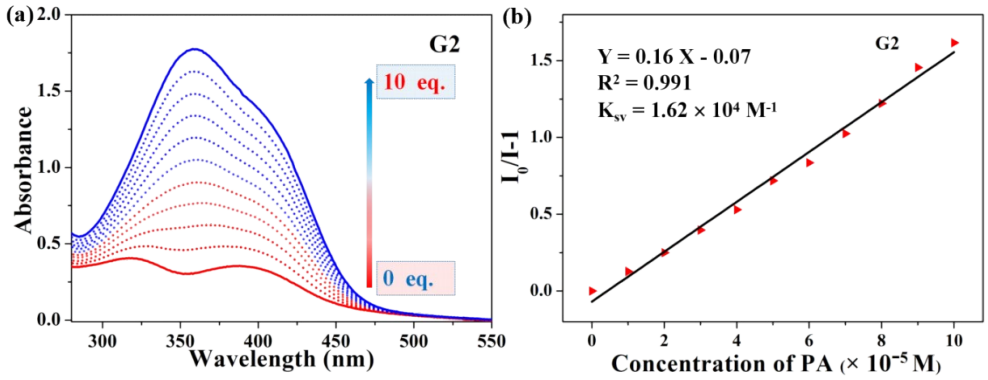

Fig. S39 (a) UV-vis spectra of G2 upn additions of PA in THF/H_2O (v/v = 1:9) mixture. (b) Corresponding Stern-Volmer plot for lower concentration of PA detection.

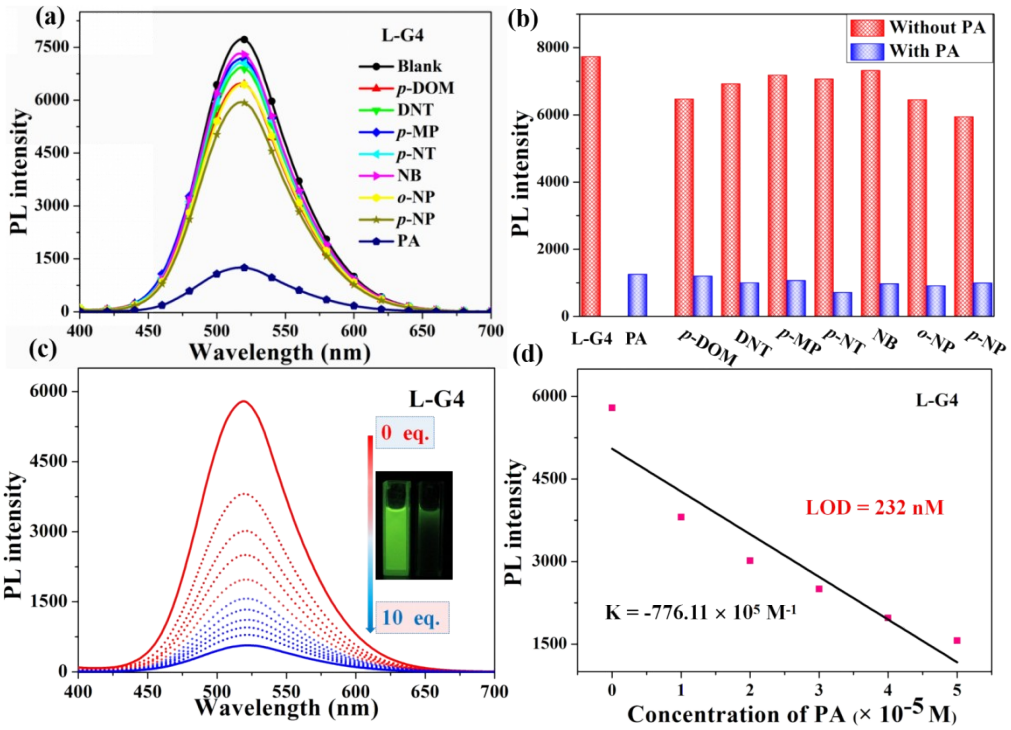

Fig. S40 (a) PL spectra response of L-G4 towards different analytes (10 equiv.) in THF/water (v/v = 1 : 9) medium; (b) quenching percentages of compound L-G4 (10.0 mM) with different analytes before (red) and (blue) after the addition of 10 equiv. (c) PL spectra of L-G4 upn additions of PA in THF/H_2O (v/v = 1:9) mixture, Inset: photos of L-G4 under UV lamp; (b) The linear relationship of L-G4 between the fluorescence intensity and the PA concentration.

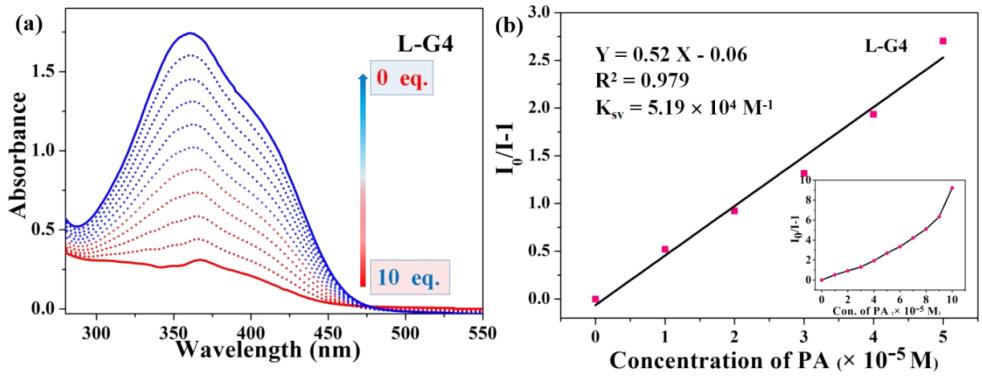

Fig. S41 (a) UV-vis spectra of L-G4 upn additions of PA in THF/H_2O (v/v = 1:9) mixture. (b) Corresponding Stern-Volmer plot for lower concentration of PA detection.

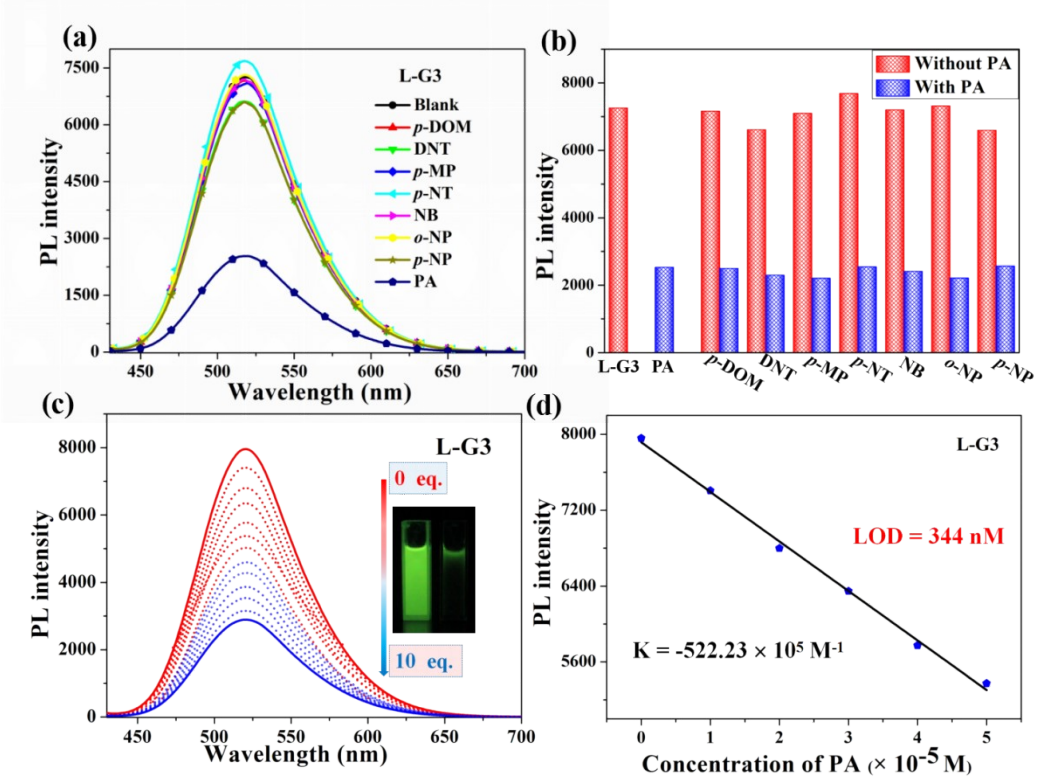

Fig. S42 (a) PL spectra response of L-G3 towards different analytes (10 equiv.) in THF/water (v/v = 1 : 9) medium; (b) quenching percentages of compound L-G3 (10.0 mM) with different analytes before (red) and (blue) after the addition of 10 equiv. (c) PL spectra of L-G3 upn additions of PA in THF/H_2O (v/v = 1:9) mixture, Inset: photos of L-G3 under UV lamp; (b) The linear relationship of L-G3 between the fluorescence intensity and the PA concentration.

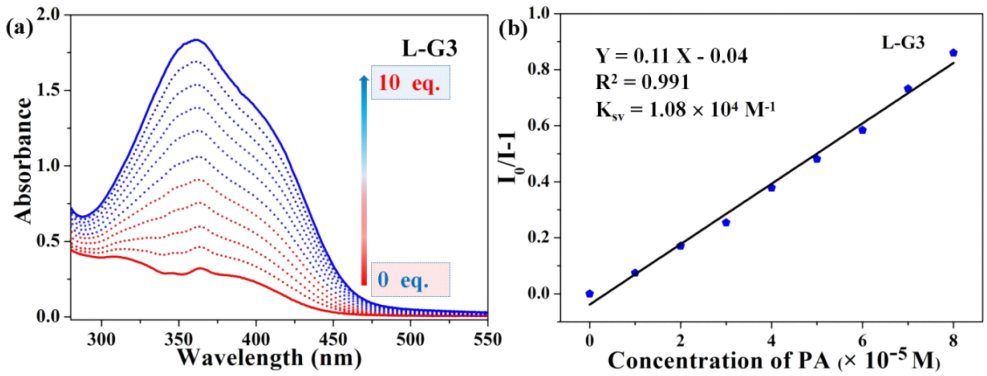

Fig. S43 (a) UV-vis spectra of L-G3 upn additions of PA in THF/H_2O (v/v = 1:9) mixture. (b) Corresponding Stern-Volmer plot for lower concentration of PA detection.

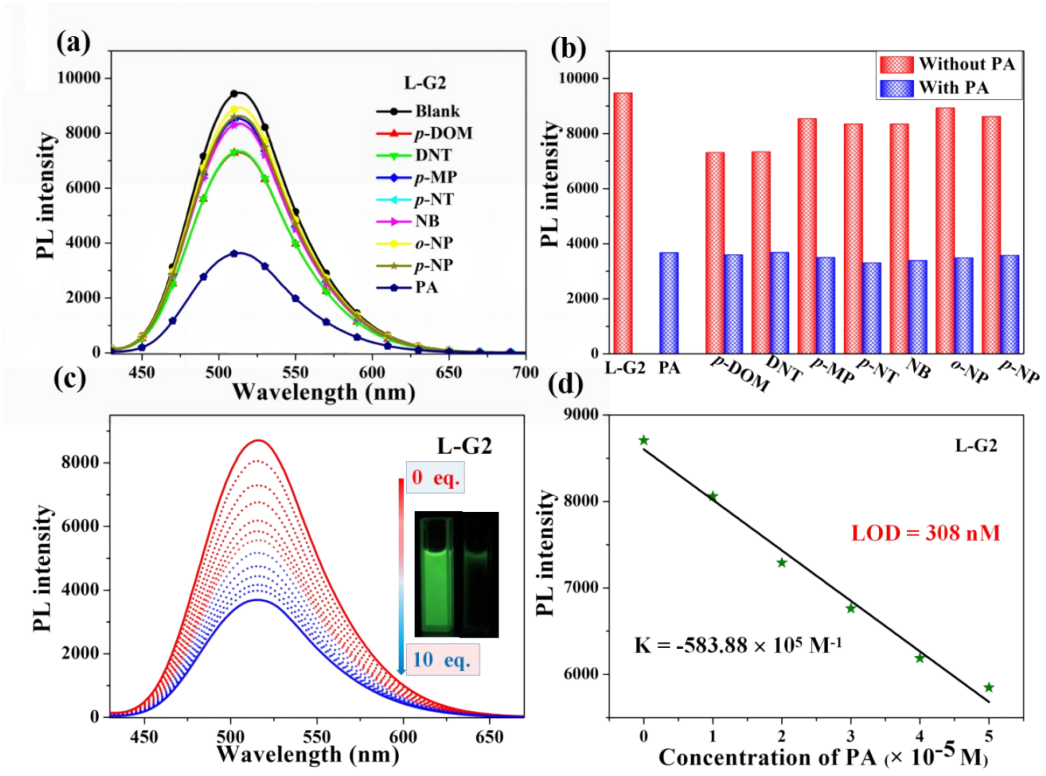

Fig. S44 (a) PL spectra response of L-G2 towards different analytes (10 equiv.) in THF/water (v/v = 1 : 9) medium; (b) quenching percentages of compound L-G2 (10.0 mM) with different analytes before (red) and (blue) after the addition of 10 equiv. (c) PL spectra of L-G2 upn additions of PA in THF/H_2O (v/v = 1:9) mixture, Inset: photos of L-G2 under UV lamp; (b) The linear relationship of L-G2 between the fluorescence intensity and the PA concentration.

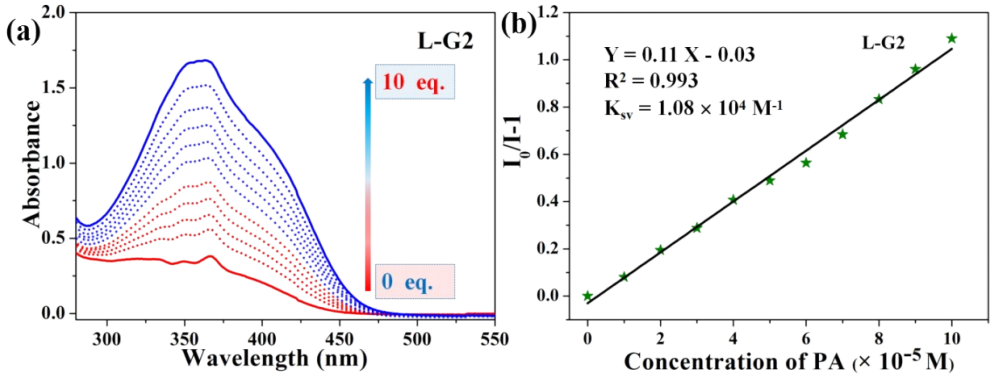

Fig. S45 (a) UV-vis spectra of **L-G2** upn additions of PA in THF/H_2O (v/v = 1:9) mixture. (b) Corresponding Stern-Volmer plot for lower concentration of PA detection.

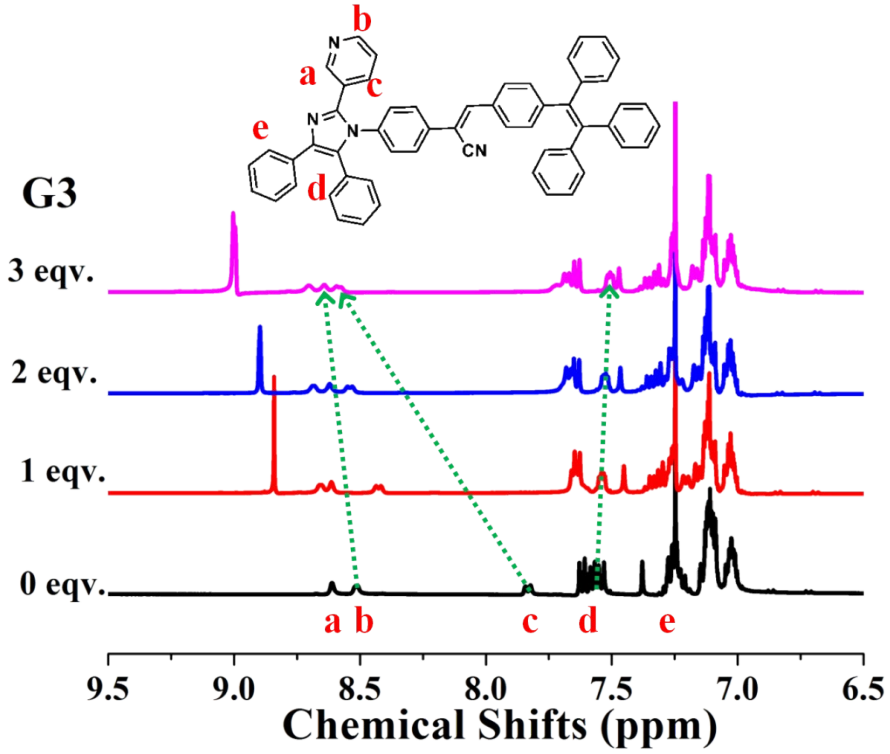

Fig. S46 Partial ^{1}H NMR titration spectra of **G3** upon addition of PA (0, 1, 2, 3 equiv.) in $CDCl_3$.

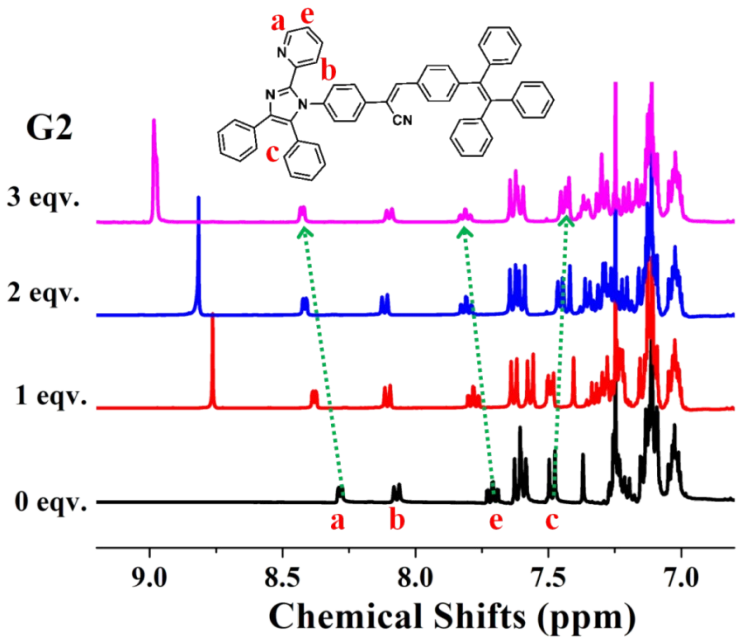

Fig. S47 Partial ^{1}H NMR titration spectra of **G2** upon addition of PA (0, 1, 2, 3 equiv.) in $CDCl_3$.

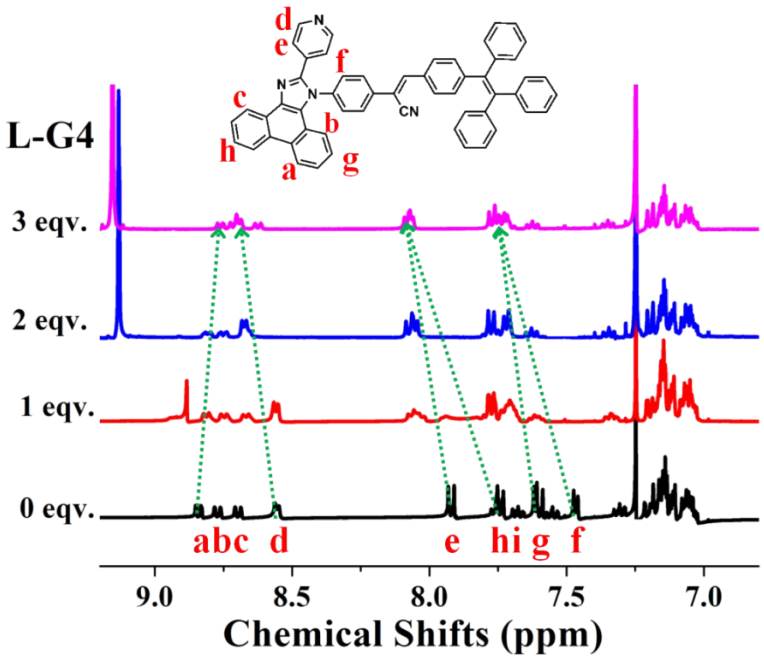

Fig. S48 Partial ^{1}H NMR titration spectra of **L-G4** upon addition of PA (0, 1, 2, 3 equiv.) in $CDCl_3$.

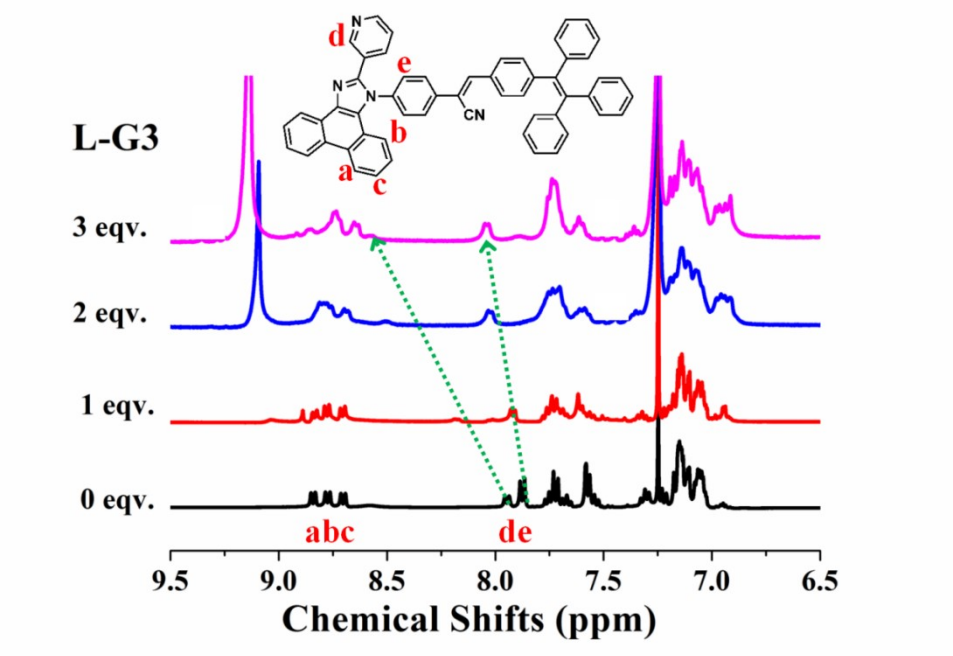

Fig. S49 Partial ^{1}H NMR titration spectra of **L-G3** upon addition of PA (0, 1, 2, 3 equiv.) in $CDCl_3$.

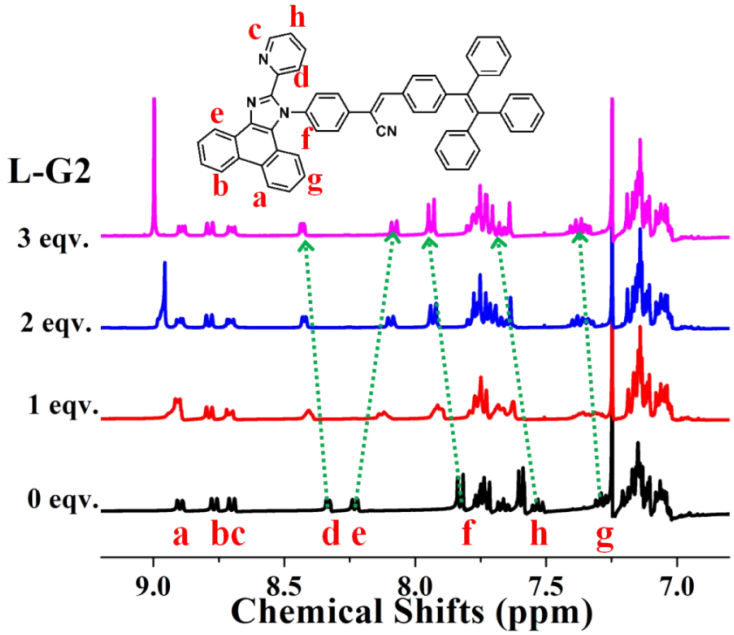

Fig. S50 Partial ^{1}H NMR titration spectra of **L-G2** upon addition of PA (0, 1, 2, 3 equiv.) in $CDCl_3$.

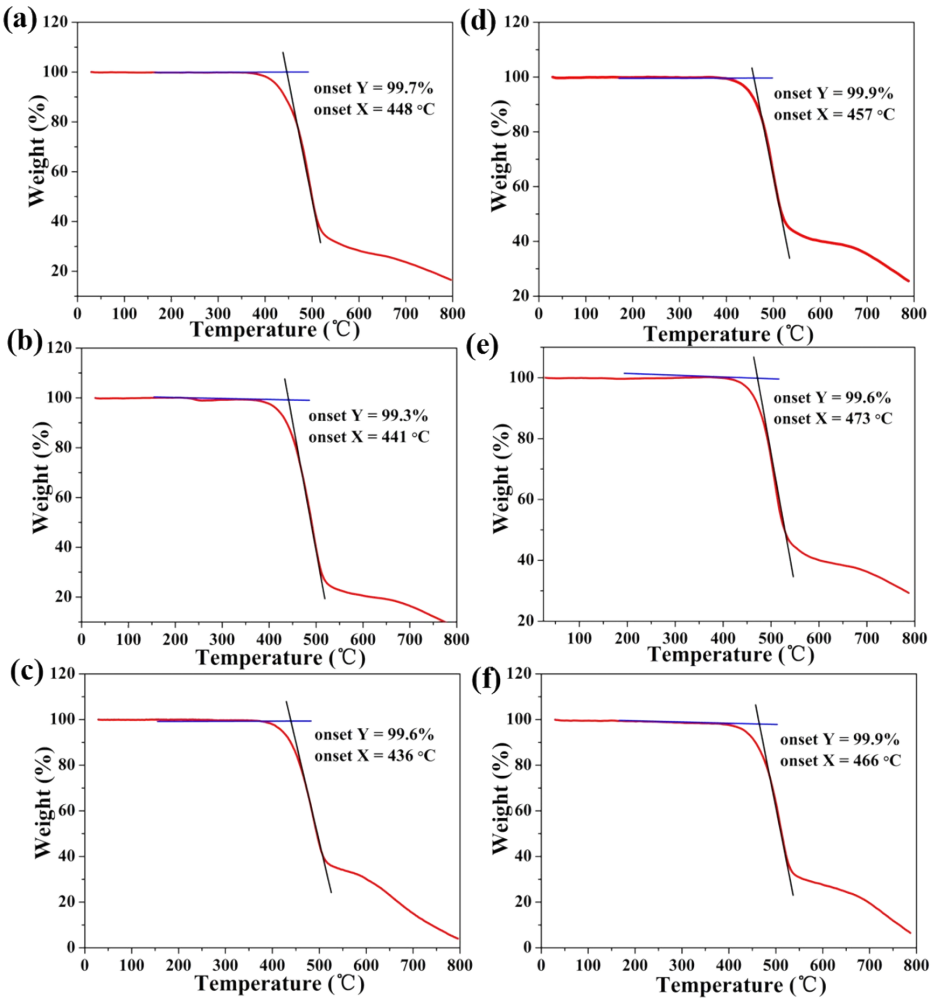

Fig. S51 TGA curve of **G4** (a), **G3** (b), **G2** (c), **L-G4** (d), **L-G3** (e), **L-G2** (f) in powders. (Scan rate: 10 °C/min)